

Isotopic Fission-Fragment Distributions as a Deep Probe to Fusion-Fission Dynamics

Fanny Farget, Manuel Caamaño

Universidade de Santiago de Compostela (Spain)

O. Delaune, X. Derkx, C. Rodríguez, C. Golabek, A. Navin, M. Rejmund, T. Roger,
M.G. Saint-Laurent, H. Savajols, C. Schmitt, C. Stodel, J.C. Thomas, A.C. Villari

GANIL (France)

D. Ramos, J. Benlliure, D. Cortina, B. Fernández

USC (Spain)

O. Tarasov, D. Bazin, W. Mittig, D.J. Morrisey, J. Pereira, B.M. Sherrill

NSCL (USA)

K.-H. Schmidt, B. Blank, S. Grévy, B. Jurado

CENBG (France)

E. Casarejos

U. de Vigo (Spain)

L. Audouin, C-O Bacri, L. Perrot

IPNO (France)

A. Heinz

U. of Chalmers (Sweden)

D. Doré, M. Delphine de Salsac

SPhN (France)

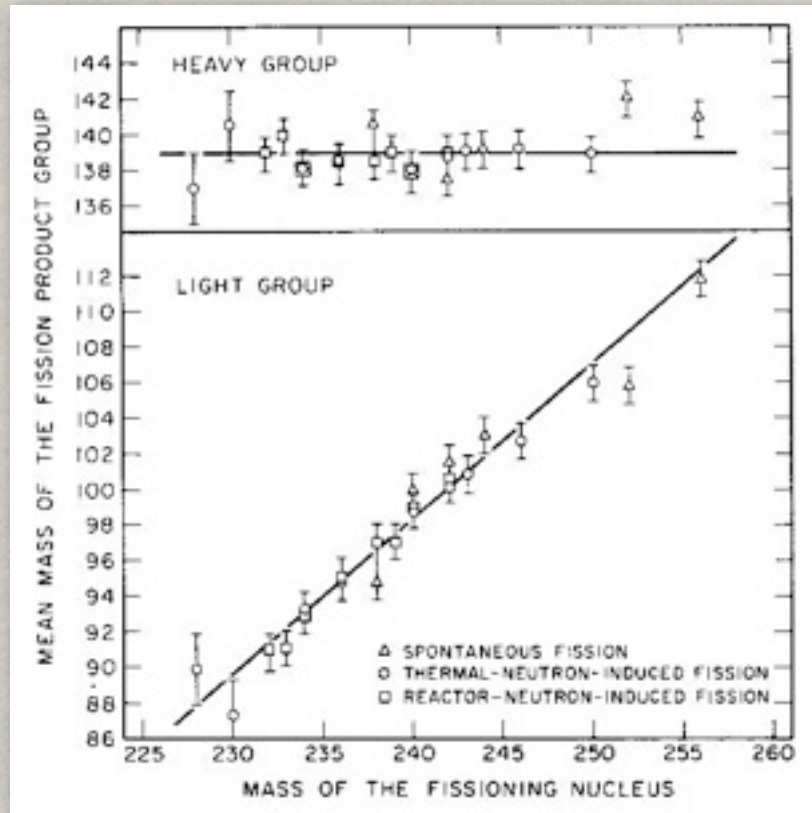
S. Lukyanov

FNLR (Russia)

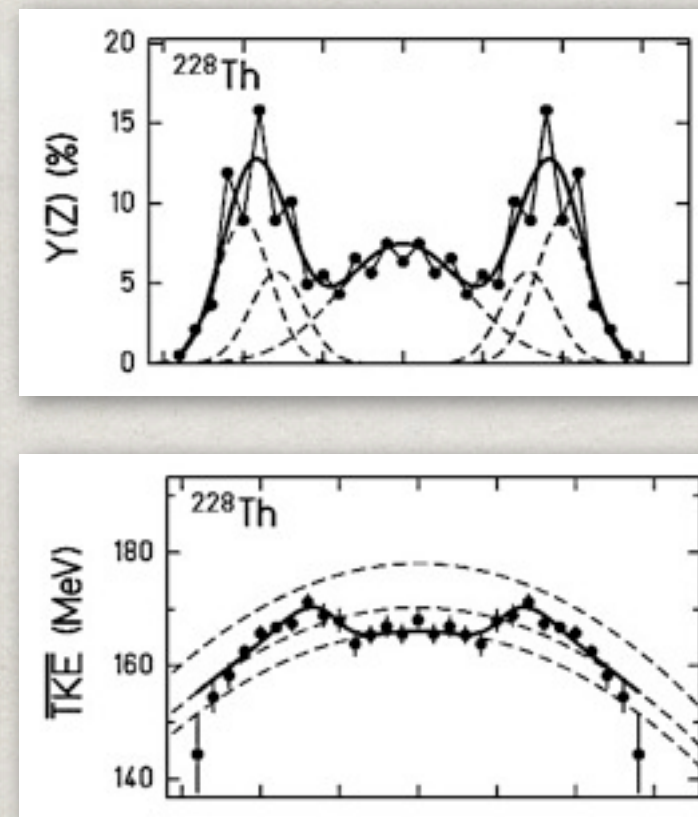
L. Gaudefroy

CEA DIF (France)

Experimental observables



K.F. Flynn *et al.* PRC 5 (1972) 1725

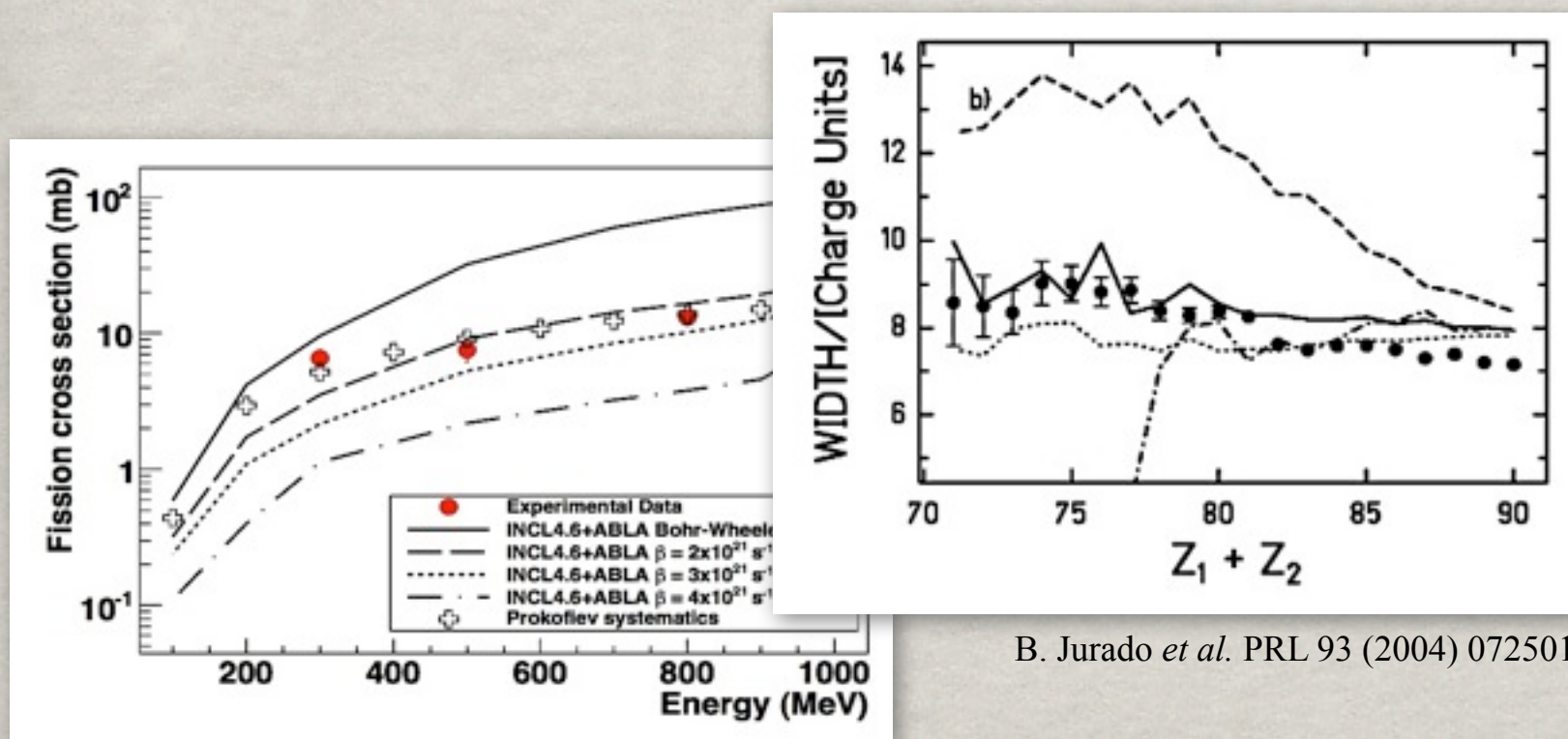


C. Böckstiegel *et al.* NPA 802 (2008) 12

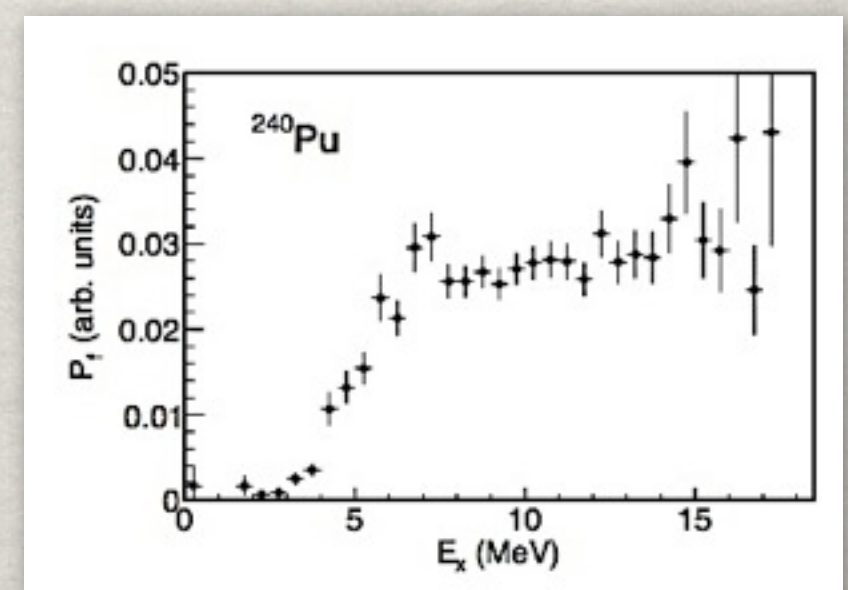
Mass, Z, and TKE showed that shell effects come into play

Measurements of fragment distributions and yields hints on the dynamics of fission

Fission probabilities reveal barrier's features



Y. Ayyad, PhD U. Santiago C (2012)



C. Rodríguez-Tajes *et al.*, to be published

Experimental observables

Different reactions grant the access to different observables and conditions

Direct kinematics

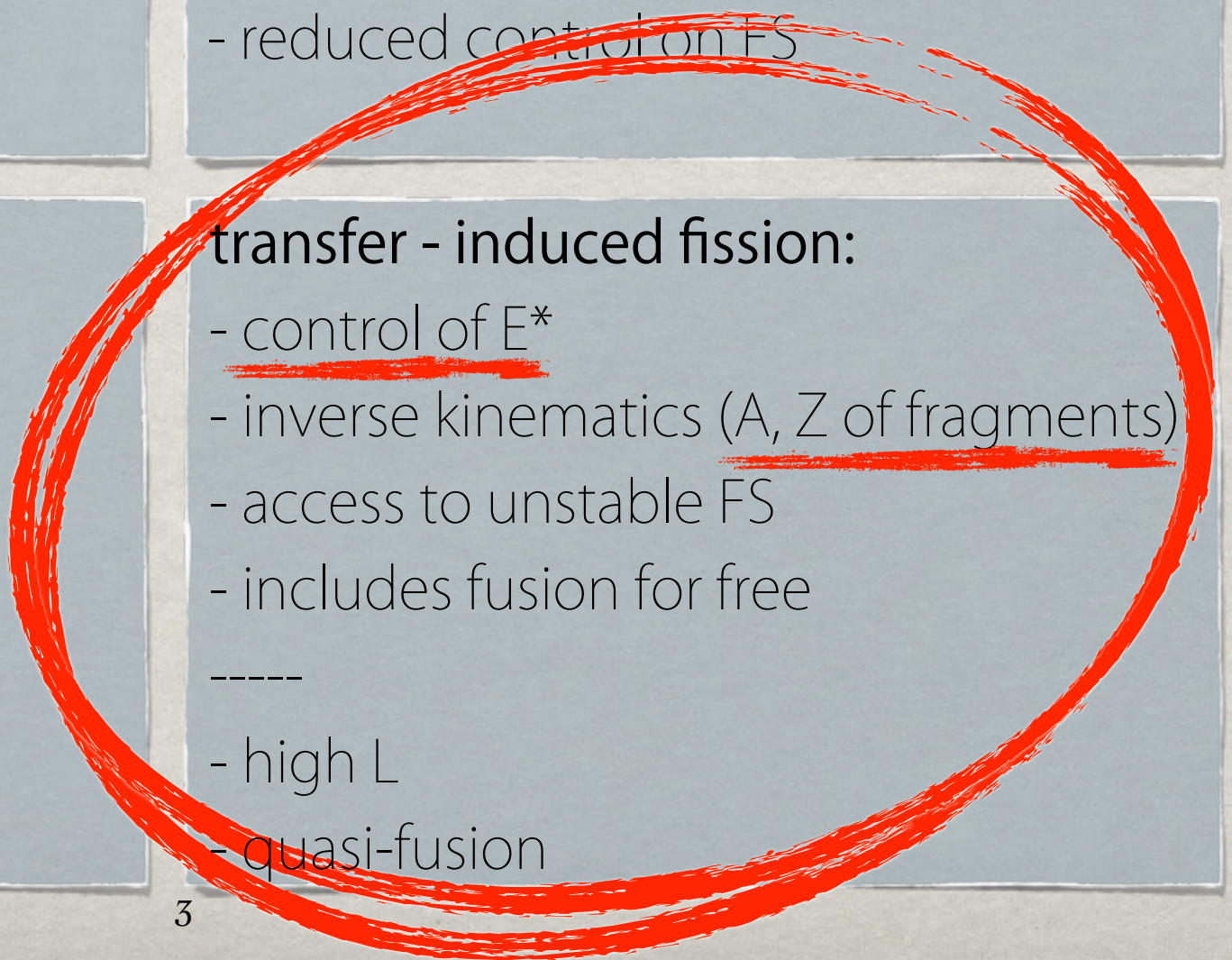
neutron - induced fission:

- control of E^*
- no high L
-
- limited to stable targets
- no access to Z

Inverse kinematics

spallation/EM - induced fission:

- inverse kinematics (A, Z of fragments)
- access to unstable FS
- no high L
-
- no control of E^*
- reduced control on FS



fusion - induced fission:

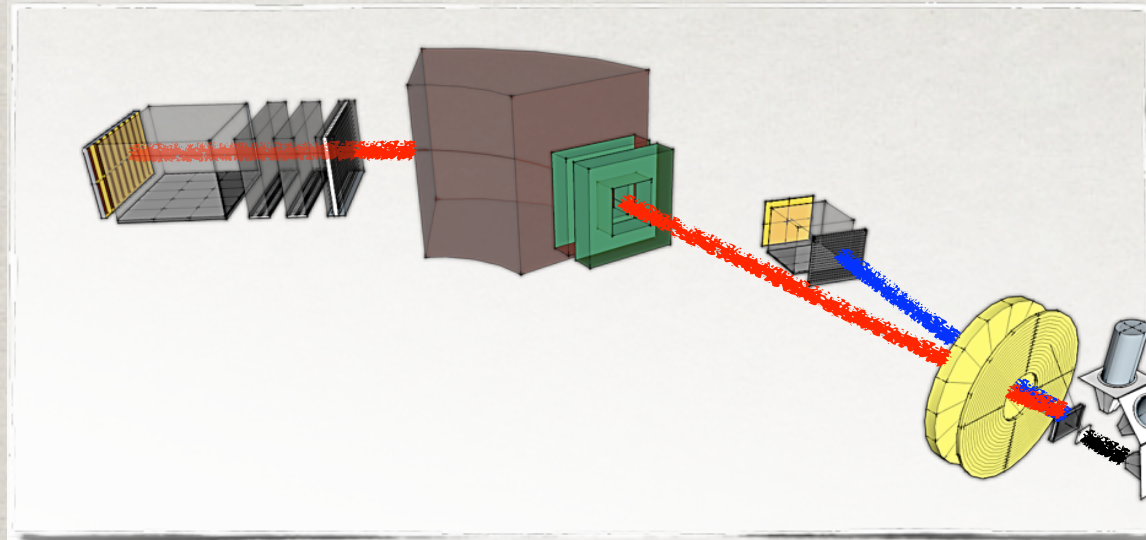
- control of E^*
- access to unstable FS
-
- high L
- quasi-fusion

transfer - induced fission:

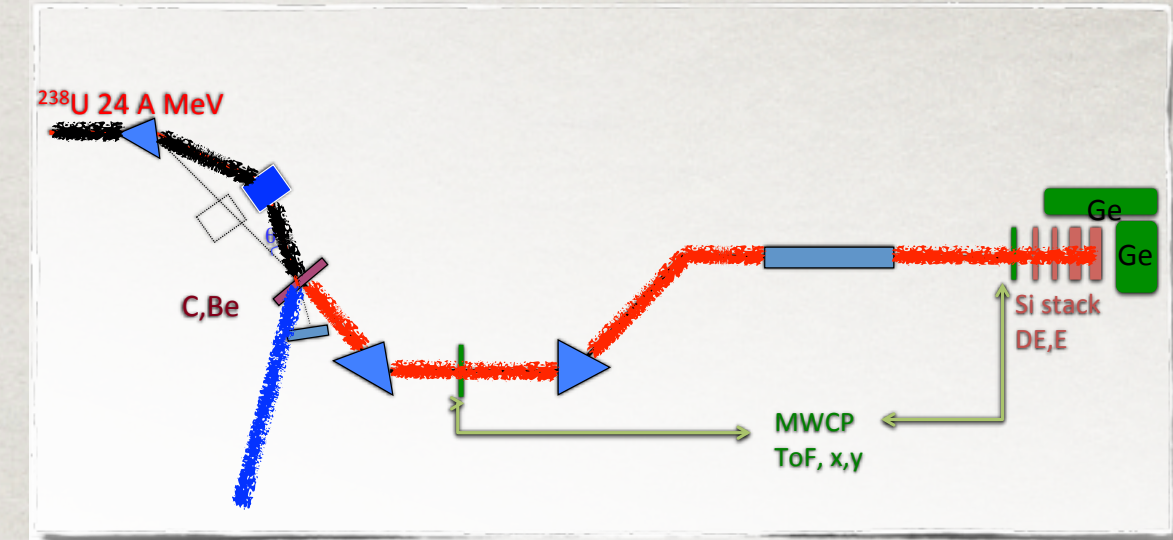
- ~~- control of E^*~~
- ~~- inverse kinematics (A, Z of fragments)~~
- access to unstable FS
- includes fusion for free
-
- high L
- quasi-fusion

Transfer/fusion-induced fission: three flavors

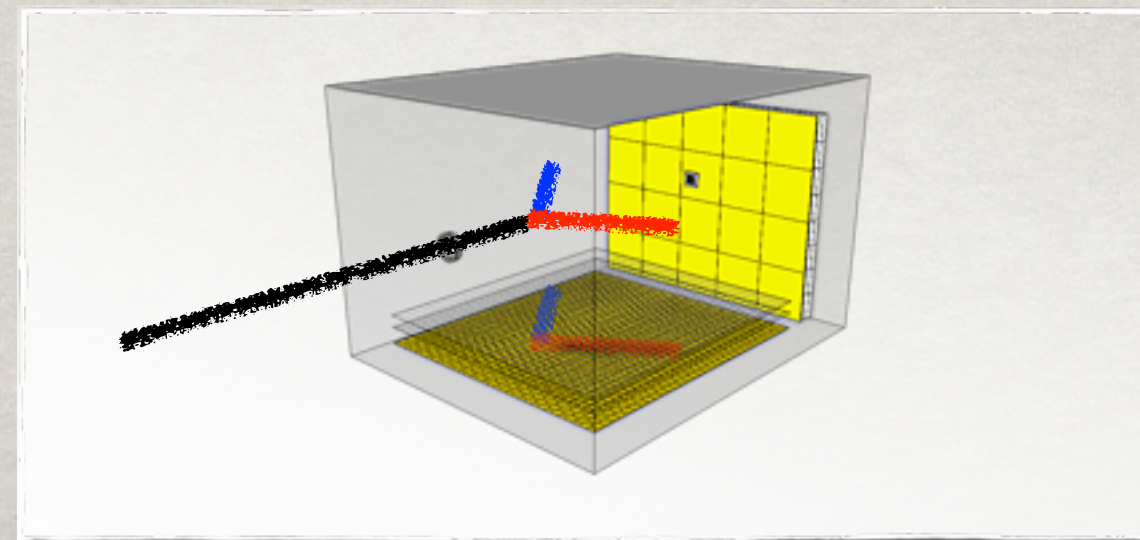
^{238}U (6.1 AMeV) + ^{12}C
at VAMOS



^{238}U (24 AMeV) + $^{12}\text{C}/^{9}\text{Be}$
at LISE

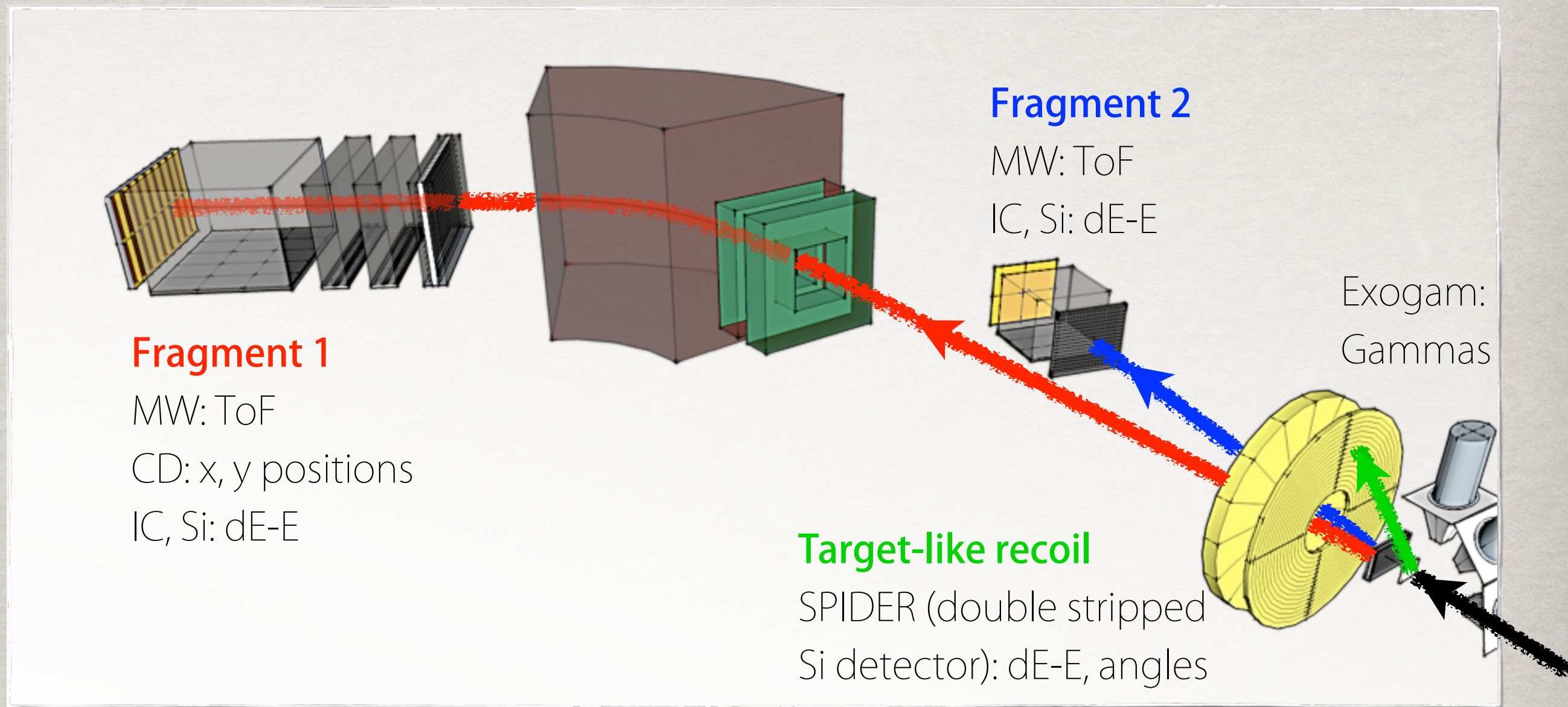


^{238}U (6 AMeV) + $^{12}\text{C}/^{2}\text{H}/^{1}\text{H}$
with MAYA



^{238}U (6.1 AMeV) + ^{12}C at VAMOS

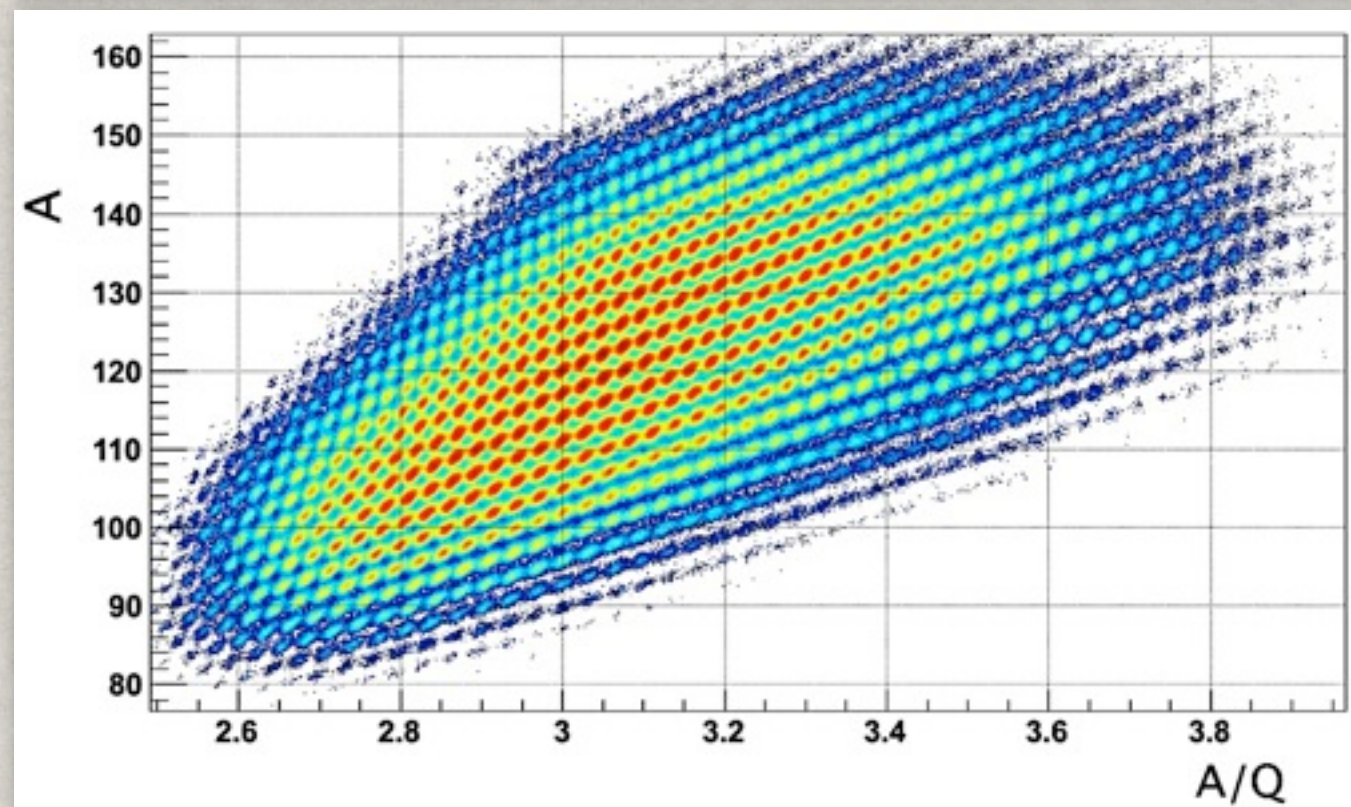
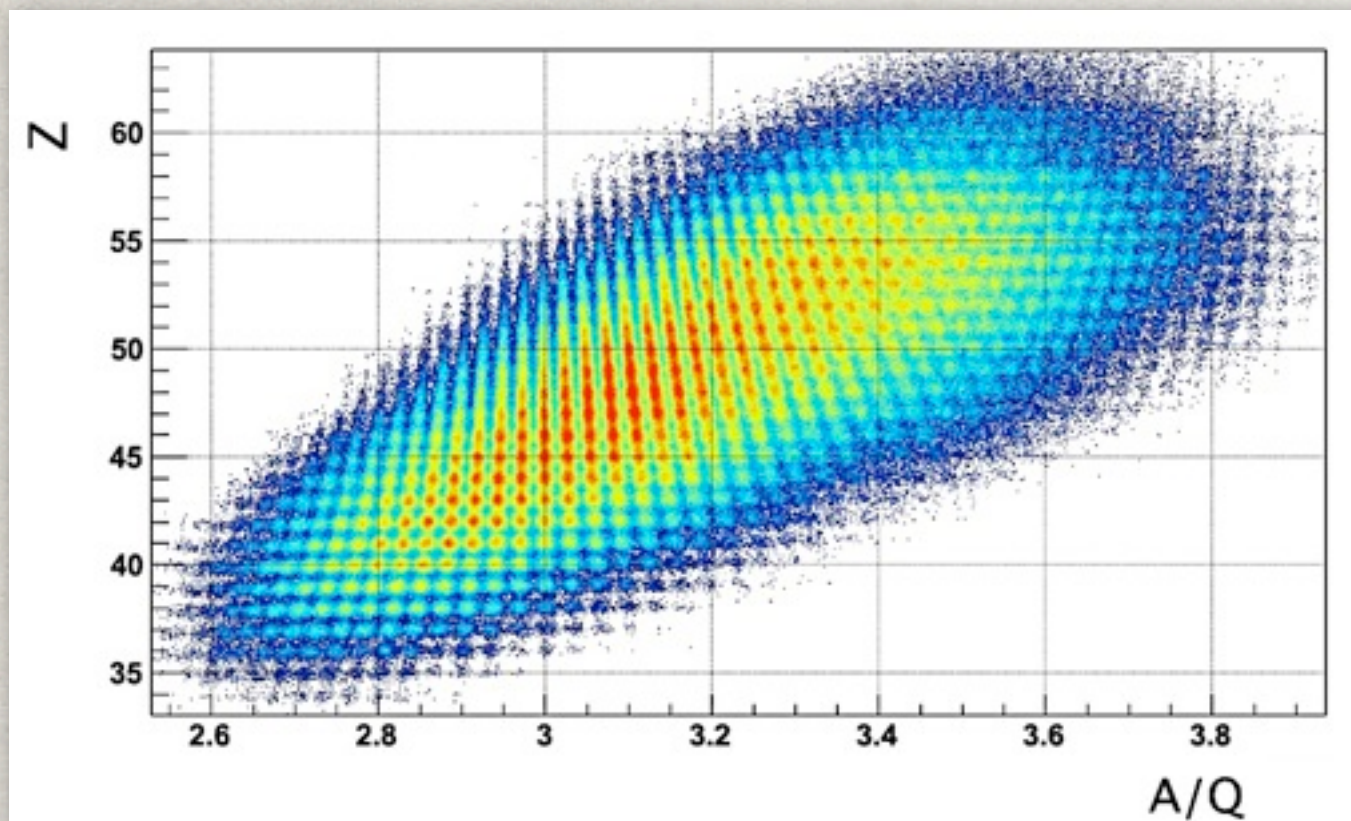
- Setup based on **inverse kinematics**
- Transfer reactions produce unstable species, induce fission.



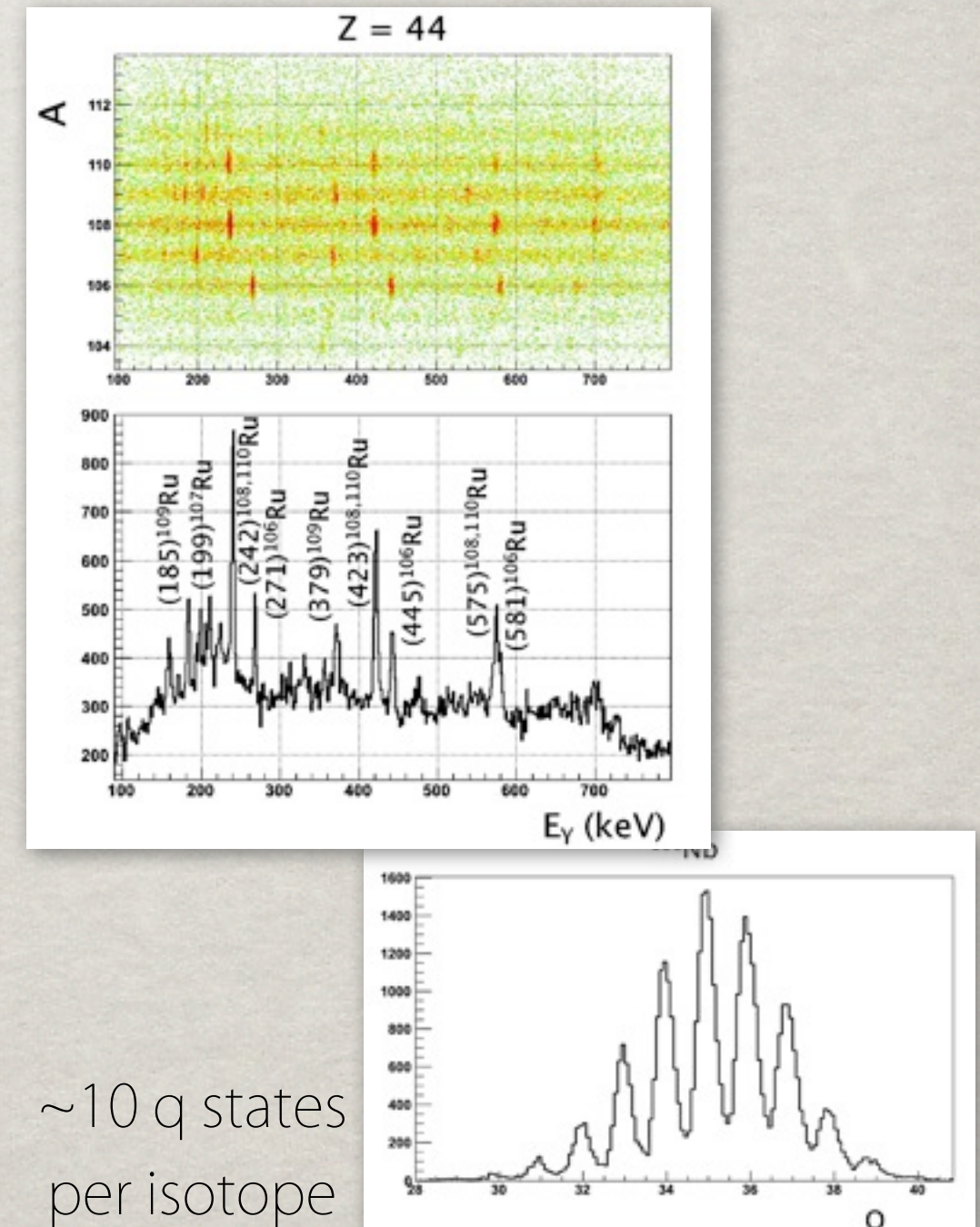
FS's observables: Z, A, E^* .

Fragments' observables: Z, A, q, angles, velocity, gammas.

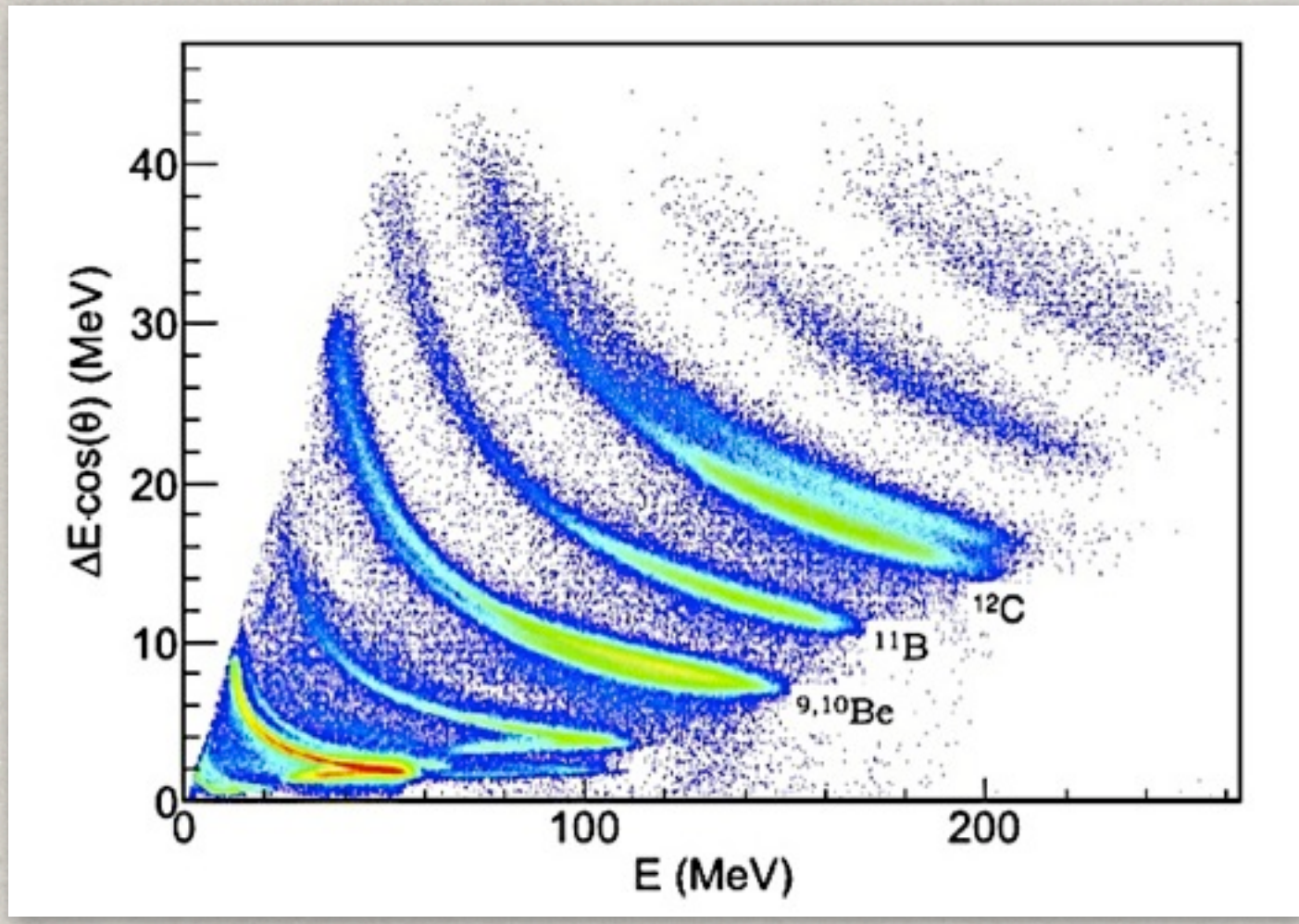
^{238}U (6.1 AMeV) + ^{12}C at VAMOS



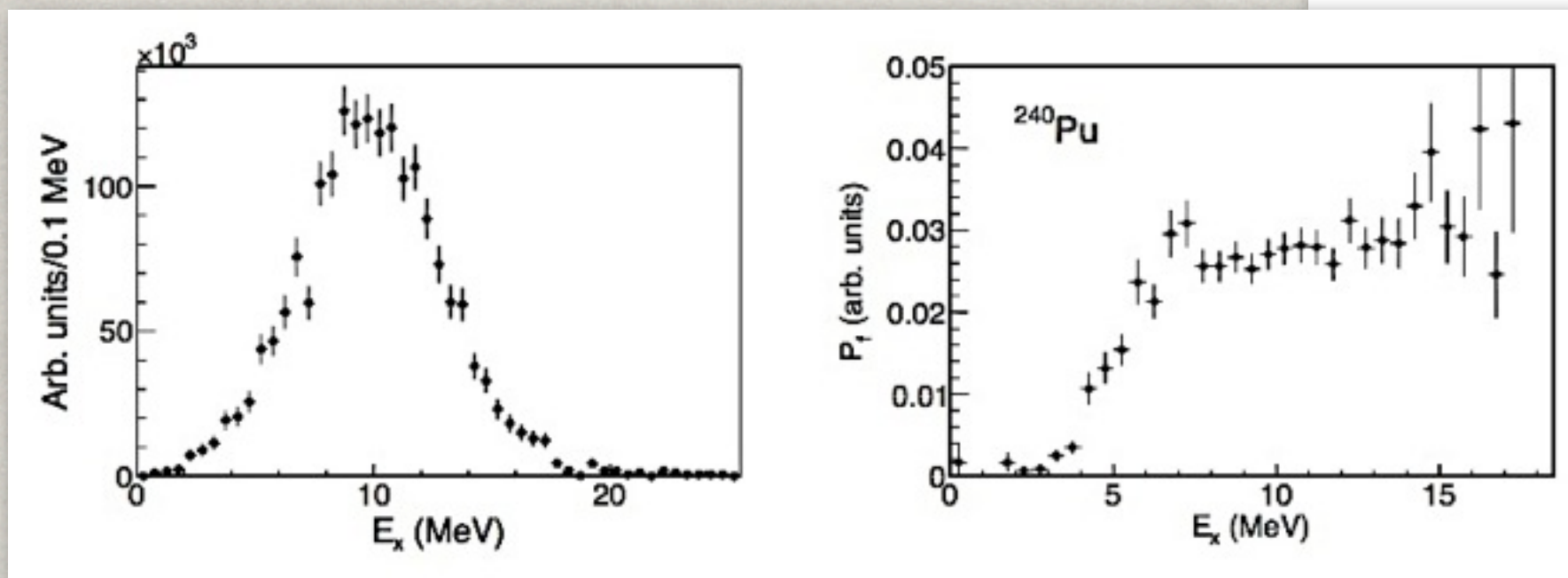
A from 80 to 160 ($\sigma/A \sim 0.3\%$)
and Z from 30 to 70 ($\sigma/Z \sim 0.9\%$)
confirmed by gamma identification.



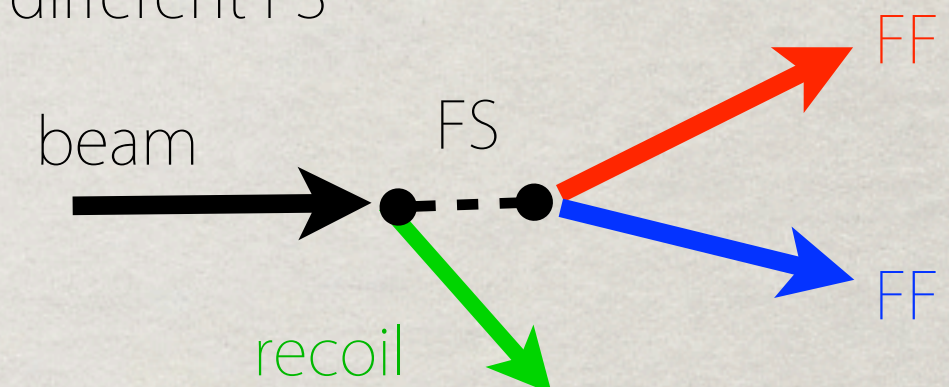
^{238}U (6.1 AMeV) + ^{12}C at VAMOS



C. Rodríguez-Tajes *et al.*, to be published



The target-like recoil tags the different FS



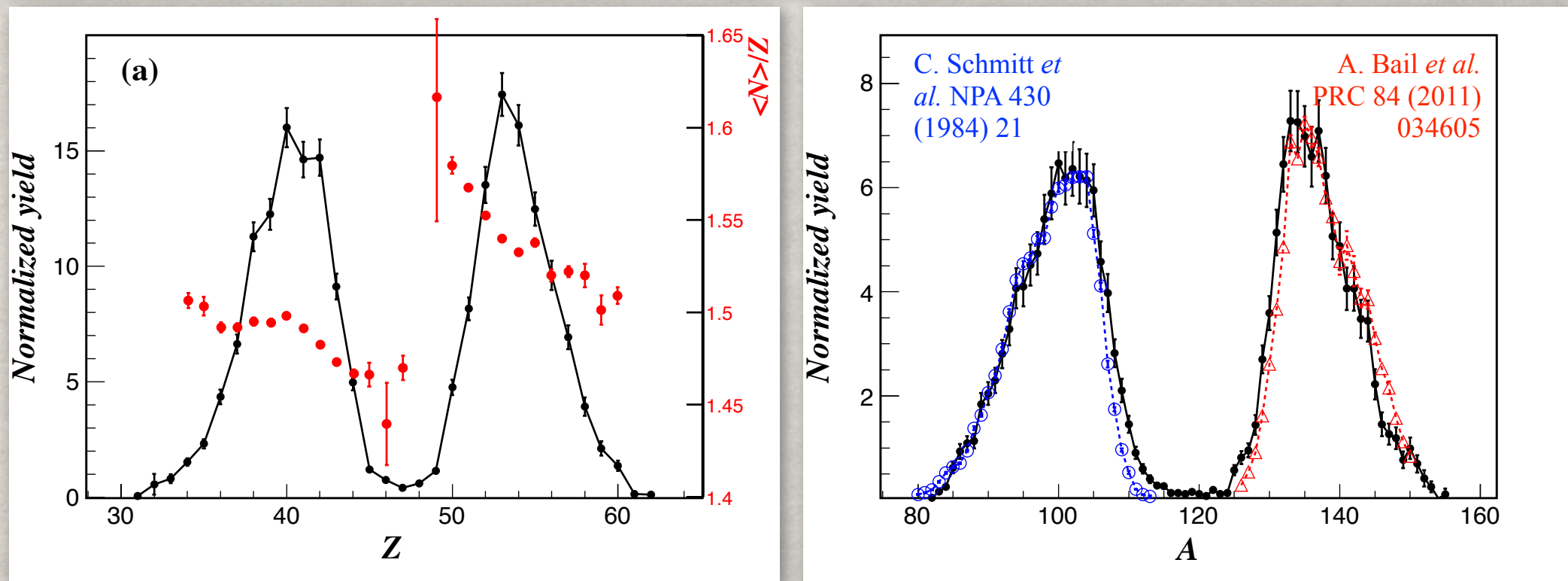
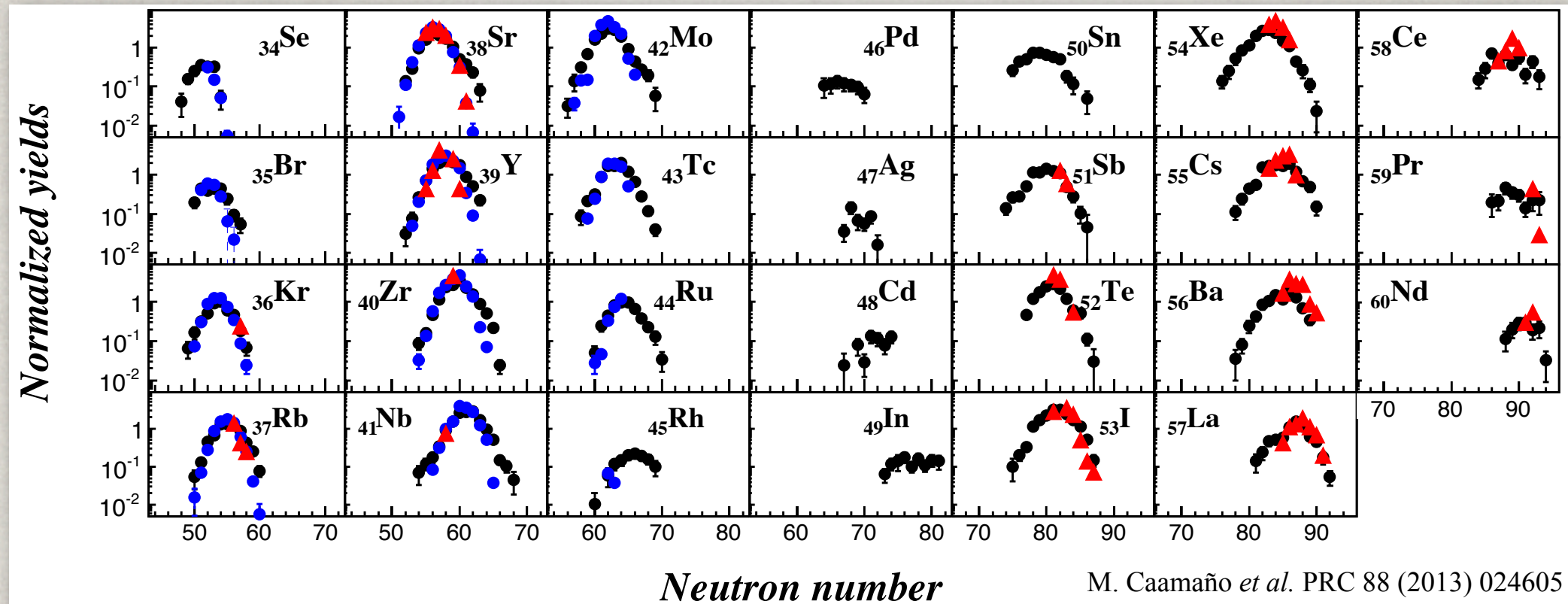
Inelastic, $E_x > 4$ MeV

- $^{12}\text{C}(^{238}\text{U}, ^{236}\text{U})^{14}\text{C}$
- $^{12}\text{C}(^{238}\text{U}, ^{239}\text{Np})^{11}\text{B}$
- $^{12}\text{C}(^{238}\text{U}, ^{240}\text{Pu})^{10}\text{Be}$
- $^{12}\text{C}(^{238}\text{U}, ^{241}\text{Pu})^9\text{Be}$
- $^{12}\text{C}(^{238}\text{U}, ^{242}\text{Pu})^8\text{Be}$
- $^{12}\text{C}(^{238}\text{U}, ^{243}\text{Am})^7\text{Li}$
- $^{12}\text{C}(^{238}\text{U}, ^{244}\text{Cm})^6\text{He}$
- $^{12}\text{C}(^{238}\text{U}, ^{246}\text{Cm})^4\text{He}$

the E^* ($\sigma \sim 1$ MeV) is deduced from kinematics.
Fission probability shows barrier's features

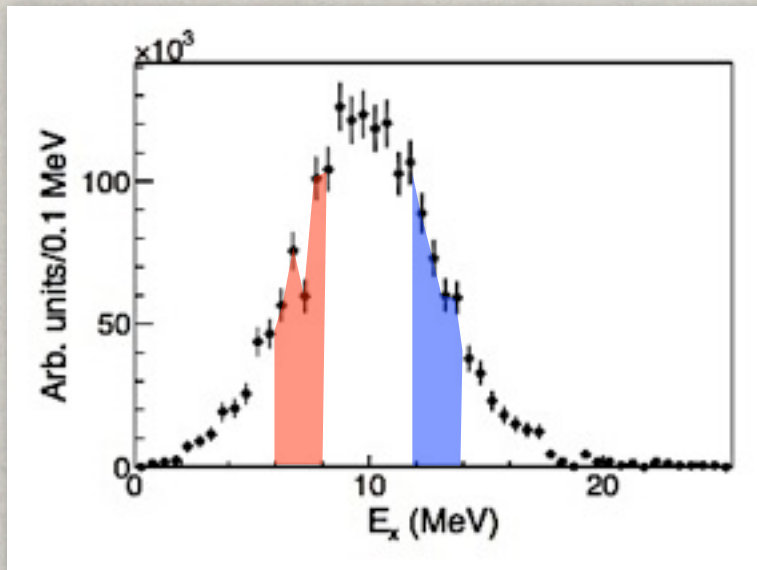
^{238}U (6.1 AMeV) + ^{12}C at VAMOS

^{12}C (^{238}U , ^{240}Pu ($E^* \sim 9$ MeV)) ^{10}Be



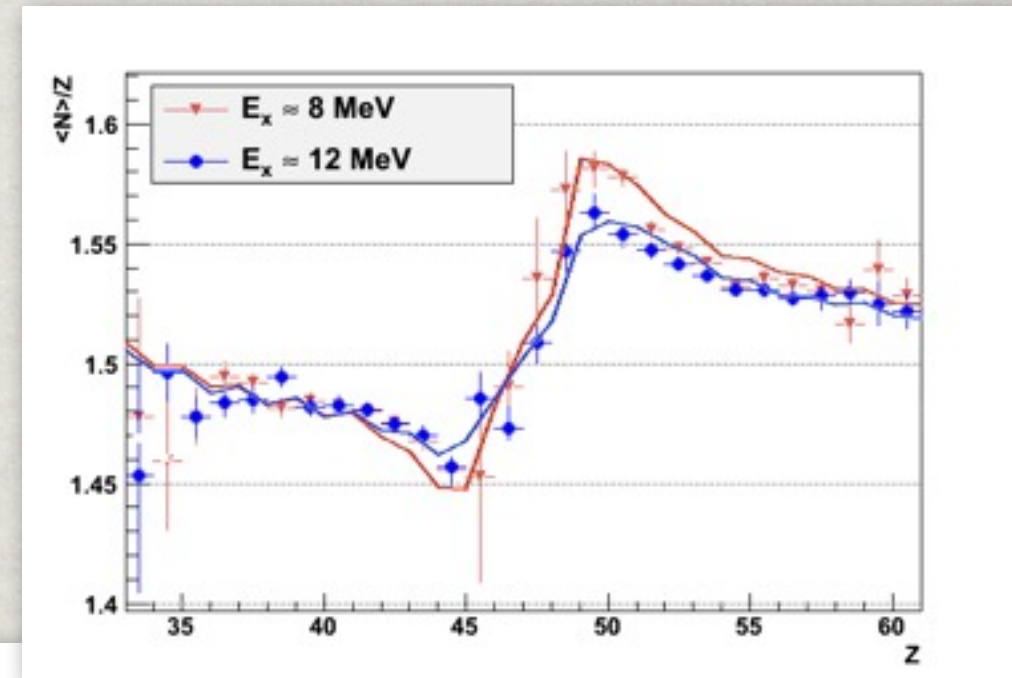
^{238}U (6.1 AMeV) + ^{12}C at VAMOS

^{240}Pu ($E^* \sim 9$ MeV)

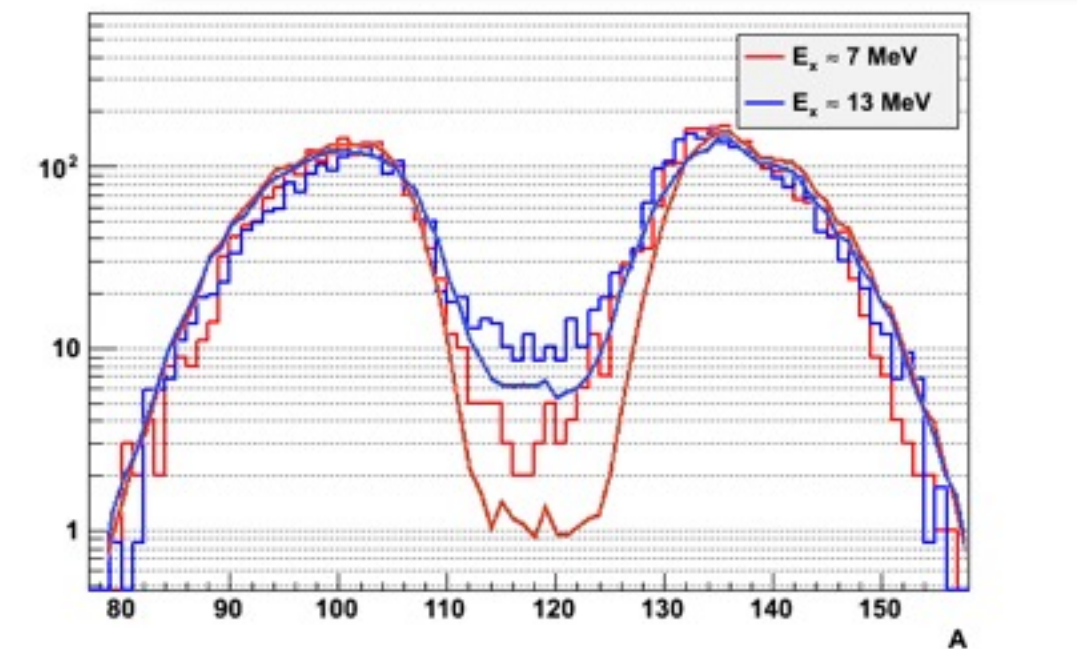
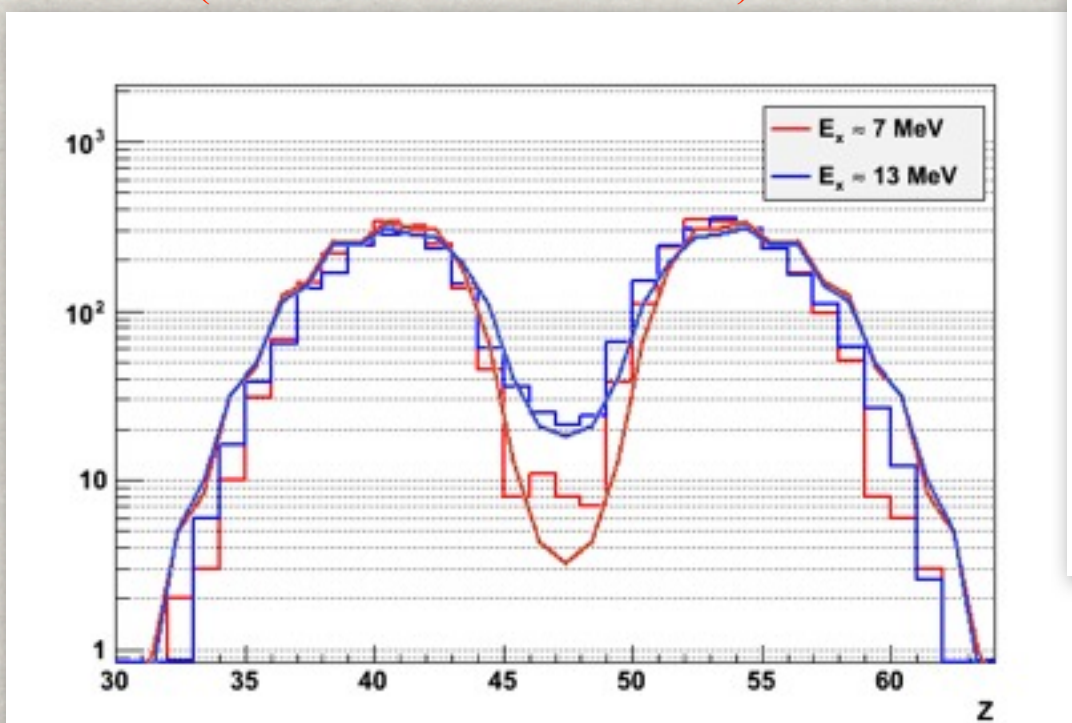


- evolution of A, Z , $\langle N \rangle/Z$ distributions with E^*

- gradual disappearance of shell effects



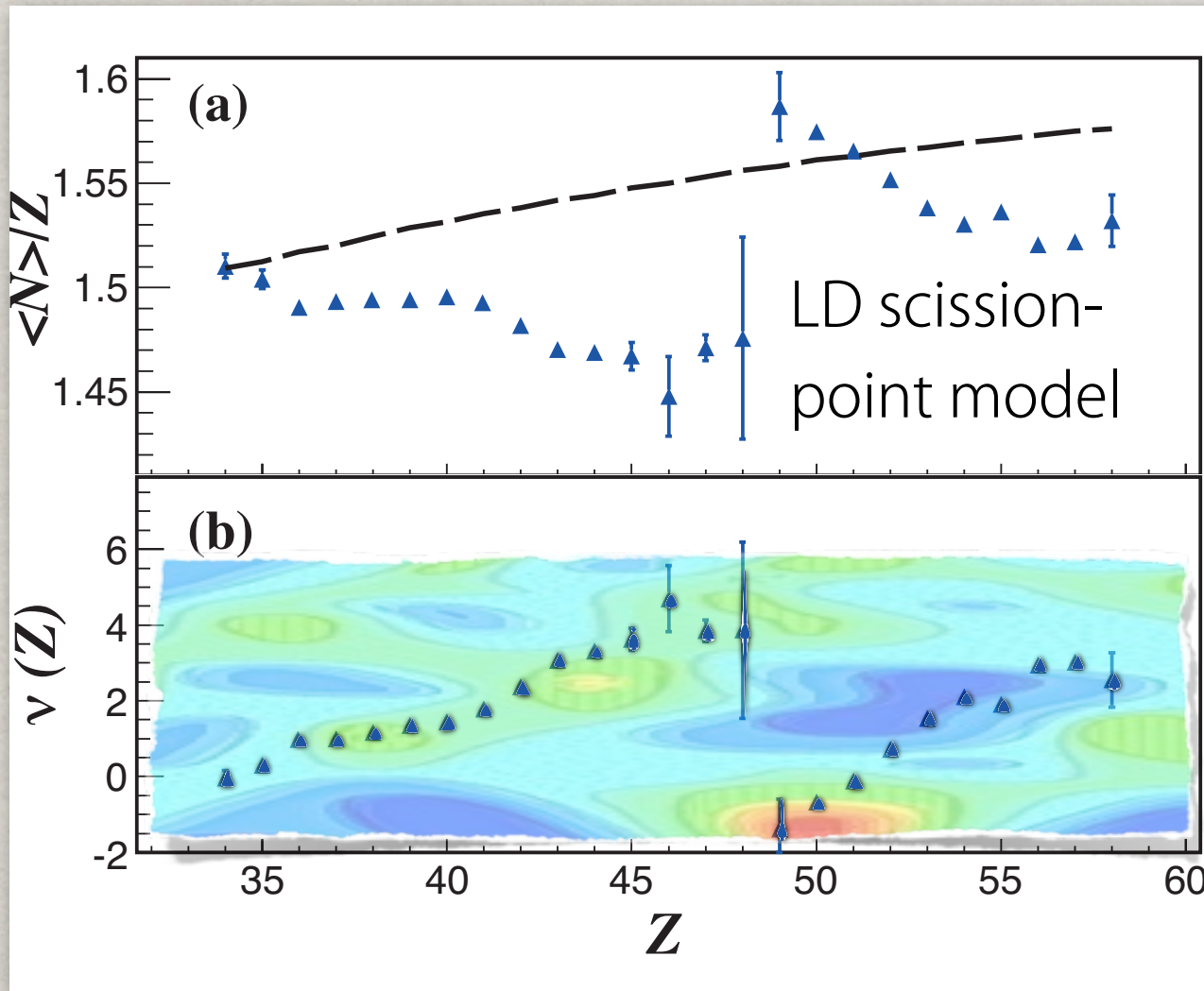
— GEF (K.-H. Schmidt & B. Jurado)



D. Ramos, PhD at U. Santiago de Compostela

^{238}U (6.1 AMeV) + ^{12}C at VAMOS

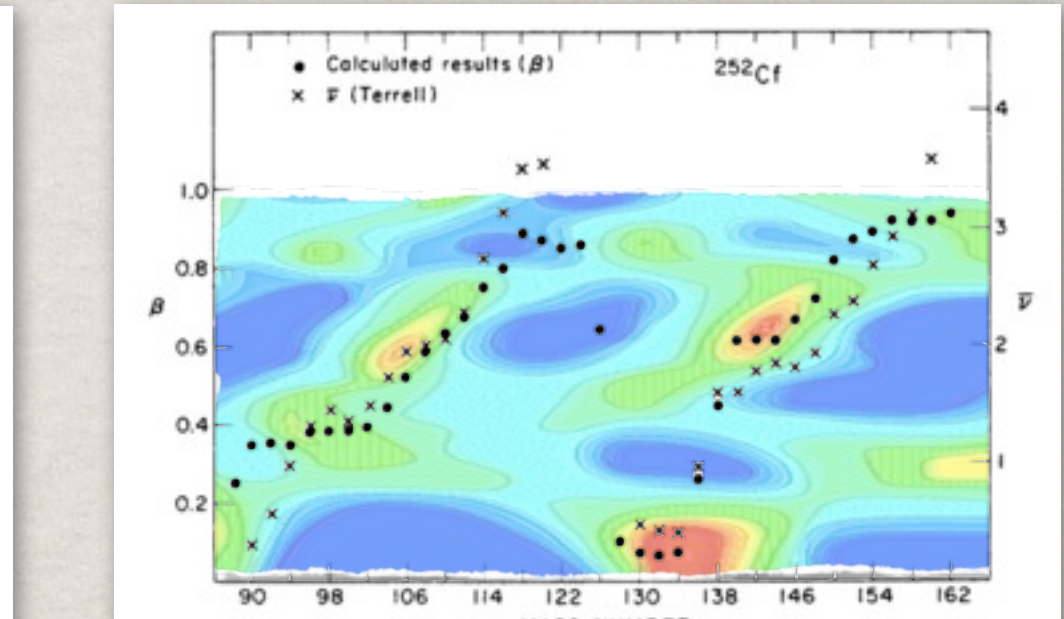
^{240}Pu ($E^* \sim 9$ MeV)



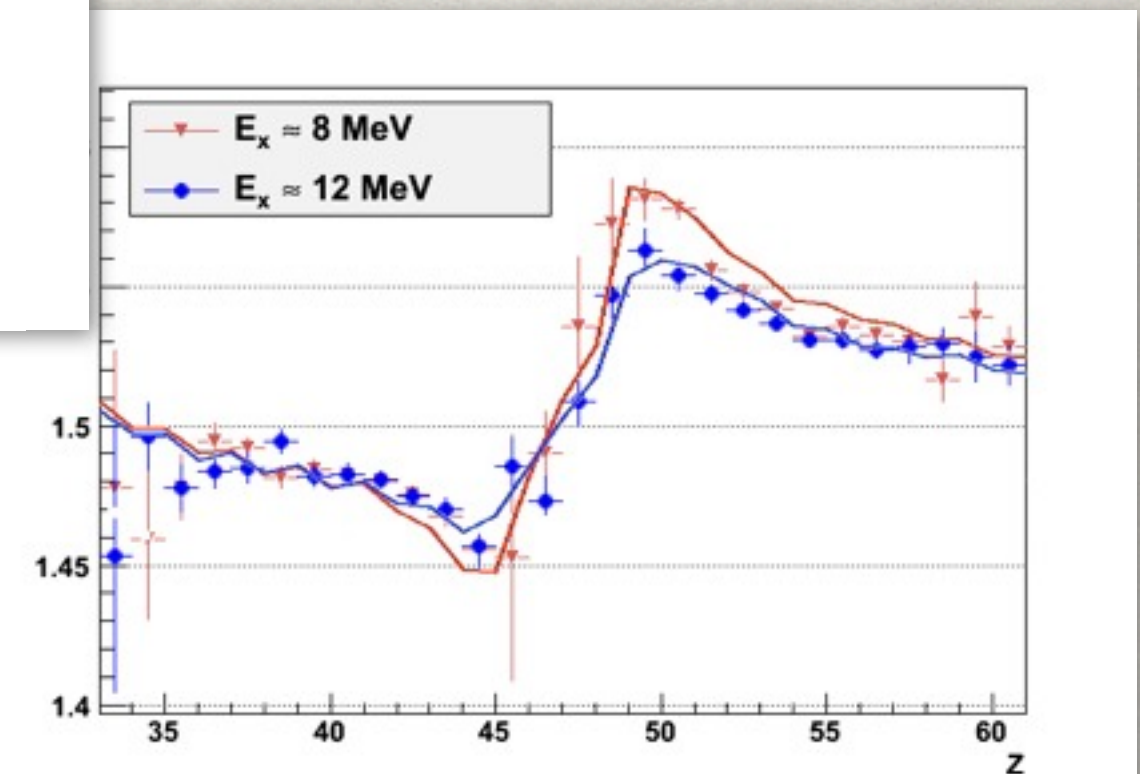
M. Caamaño *et al.* PRC 88 (2013) 024605

LD scission-point model
 $E_{\text{tot}} = E_{\text{LD}}(Z_1, A_1) + E_{\text{LD}}(Z_2, A_2)$

the obtained results can be linked to deformed shell effects



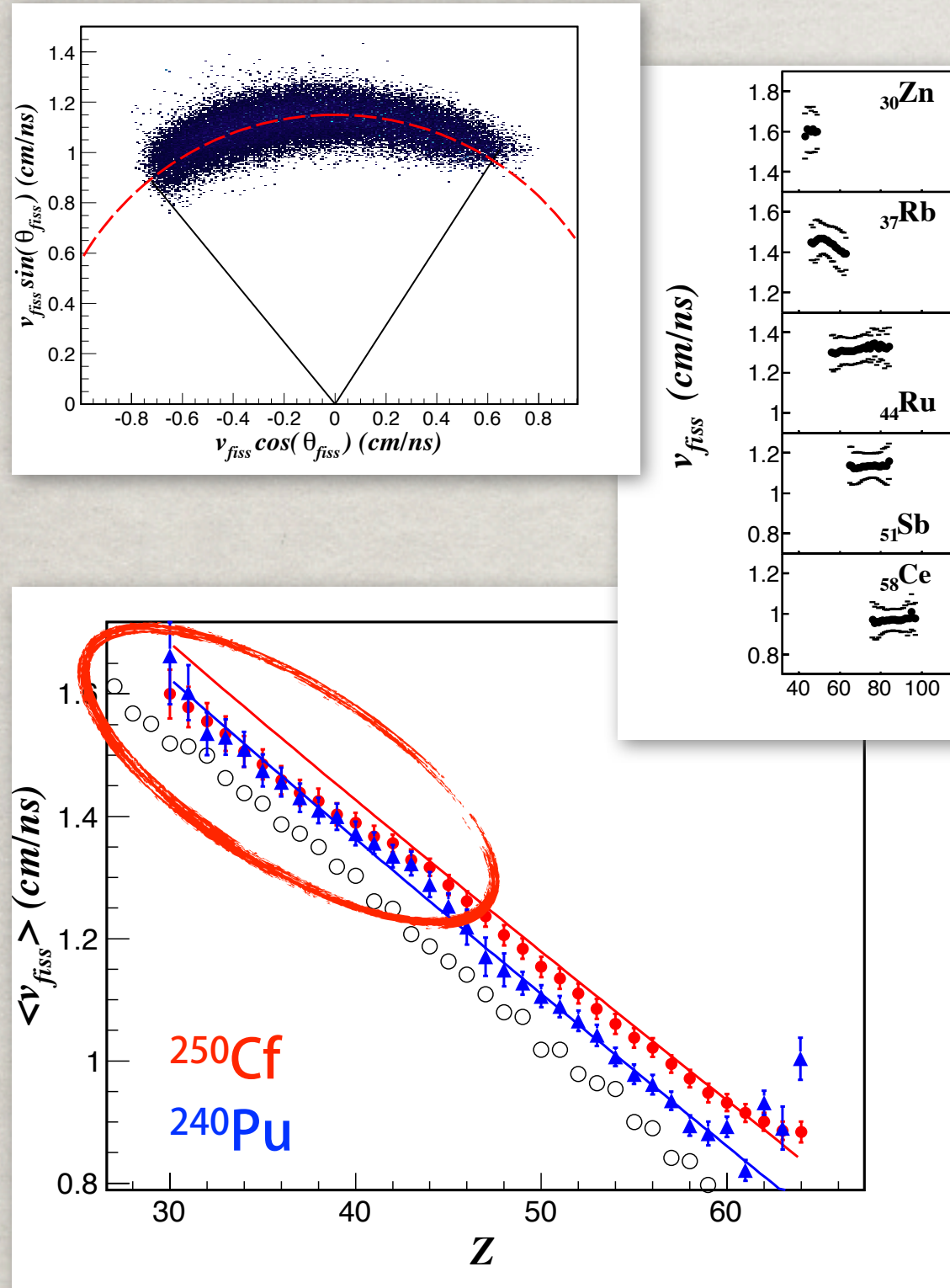
B.D. Wilkins *et al.* PRC 14 (1976) 1832



D. Ramos, PhD at U. Santiago de Compostela

^{238}U (6.1 AMeV) + ^{12}C at VAMOS

^{240}Pu ($E^* \sim 9$ MeV)

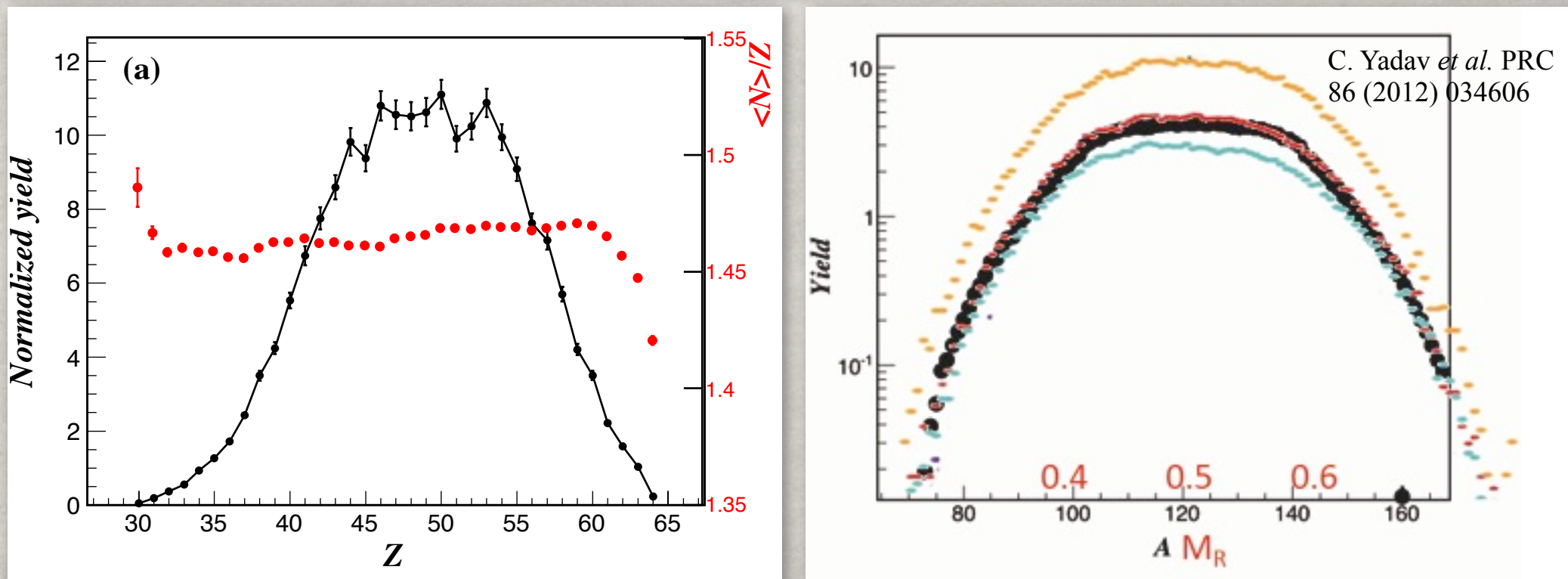
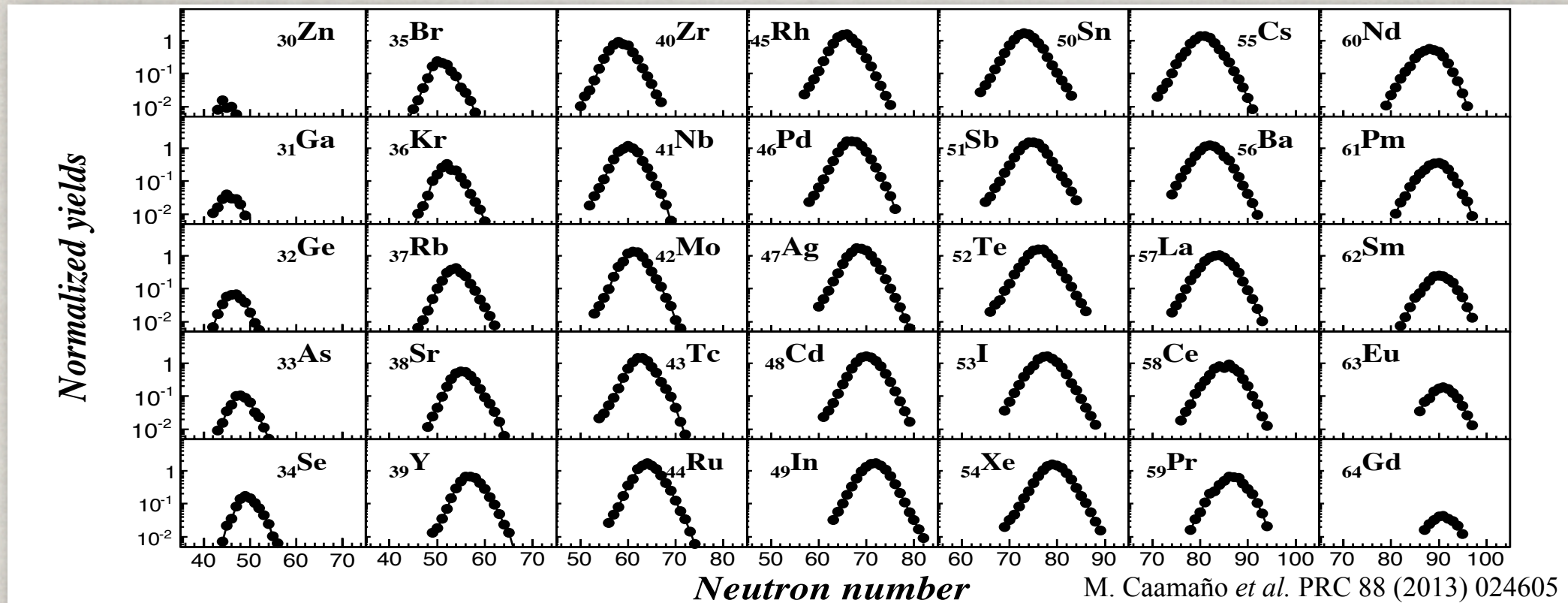


M. Caamaño *et al.* PRC 88 (2013) 024605

The fragments' velocities are also available.
 ^{240}Pu follows the systematics of Wilkins.
 ^{250}Cf deviates at light fragments.

^{238}U (6.1 AMeV) + ^{12}C at VAMOS

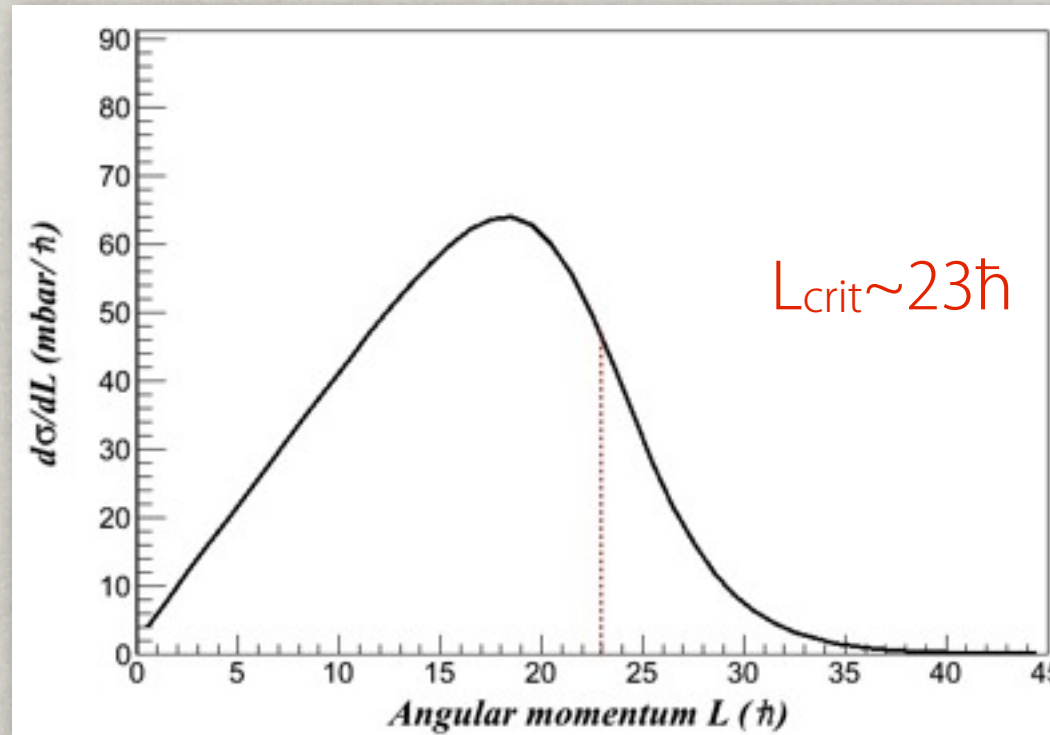
^{12}C (^{238}U , ^{250}Cf ($E^* \sim 45$ MeV))



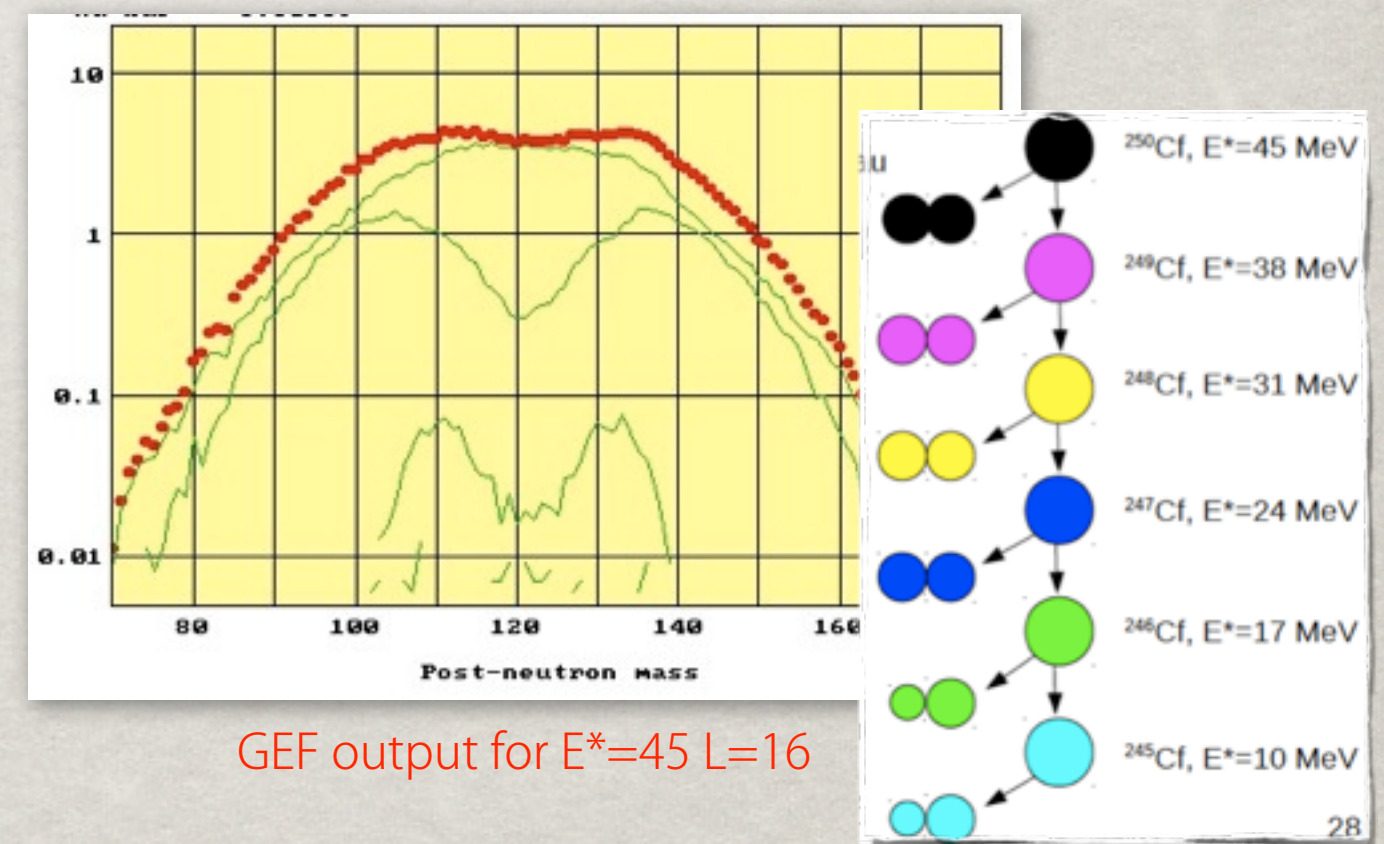
^{238}U (6.1 AMeV) + ^{12}C at VAMOS

^{250}Cf ($E^* \sim 45$ MeV)

Fusion-fission reaction:
angular momentum distribution

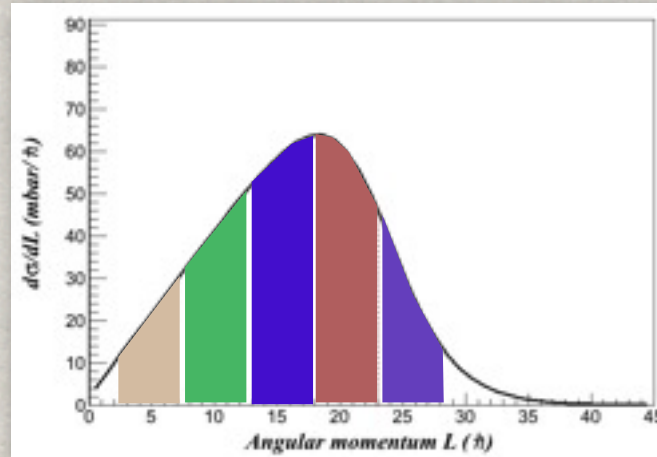


High excitation energy:
multi-chance fission

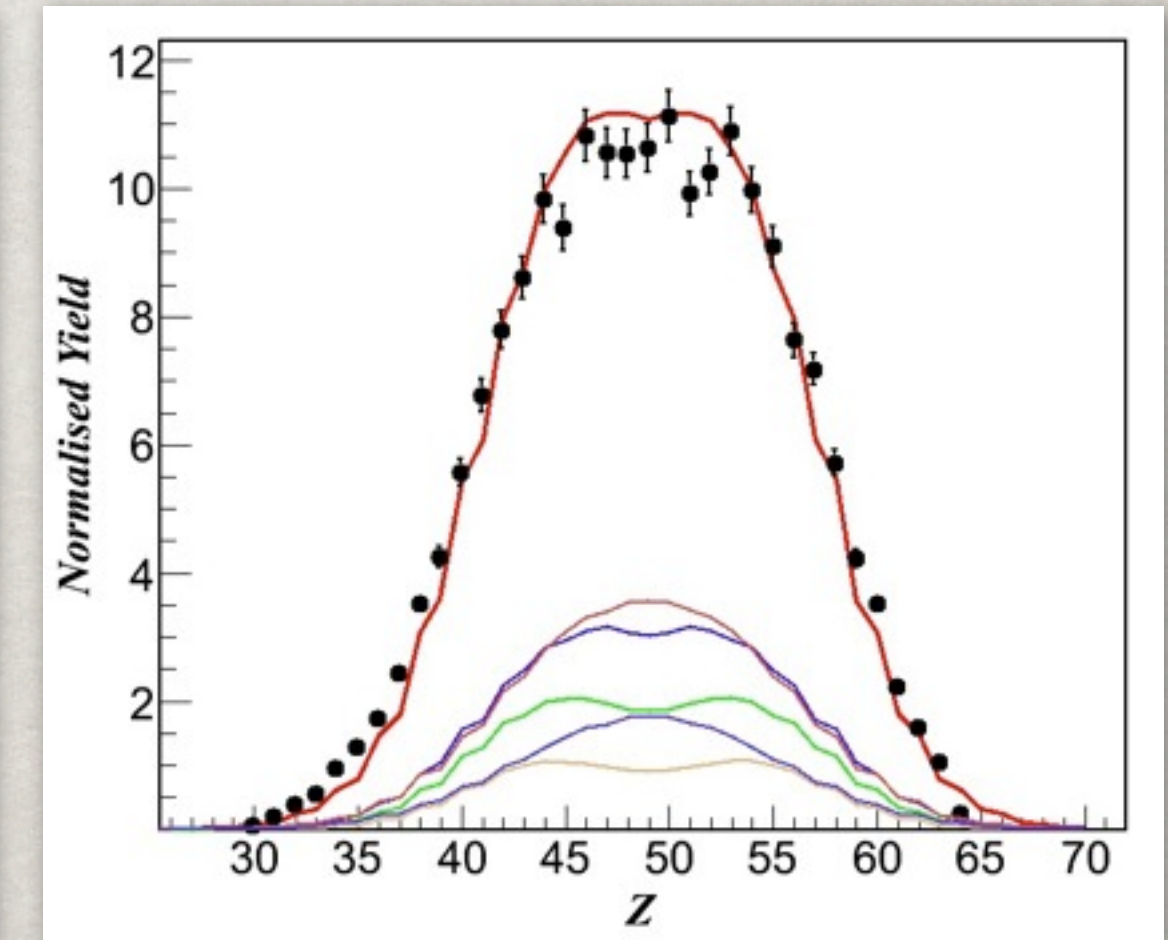
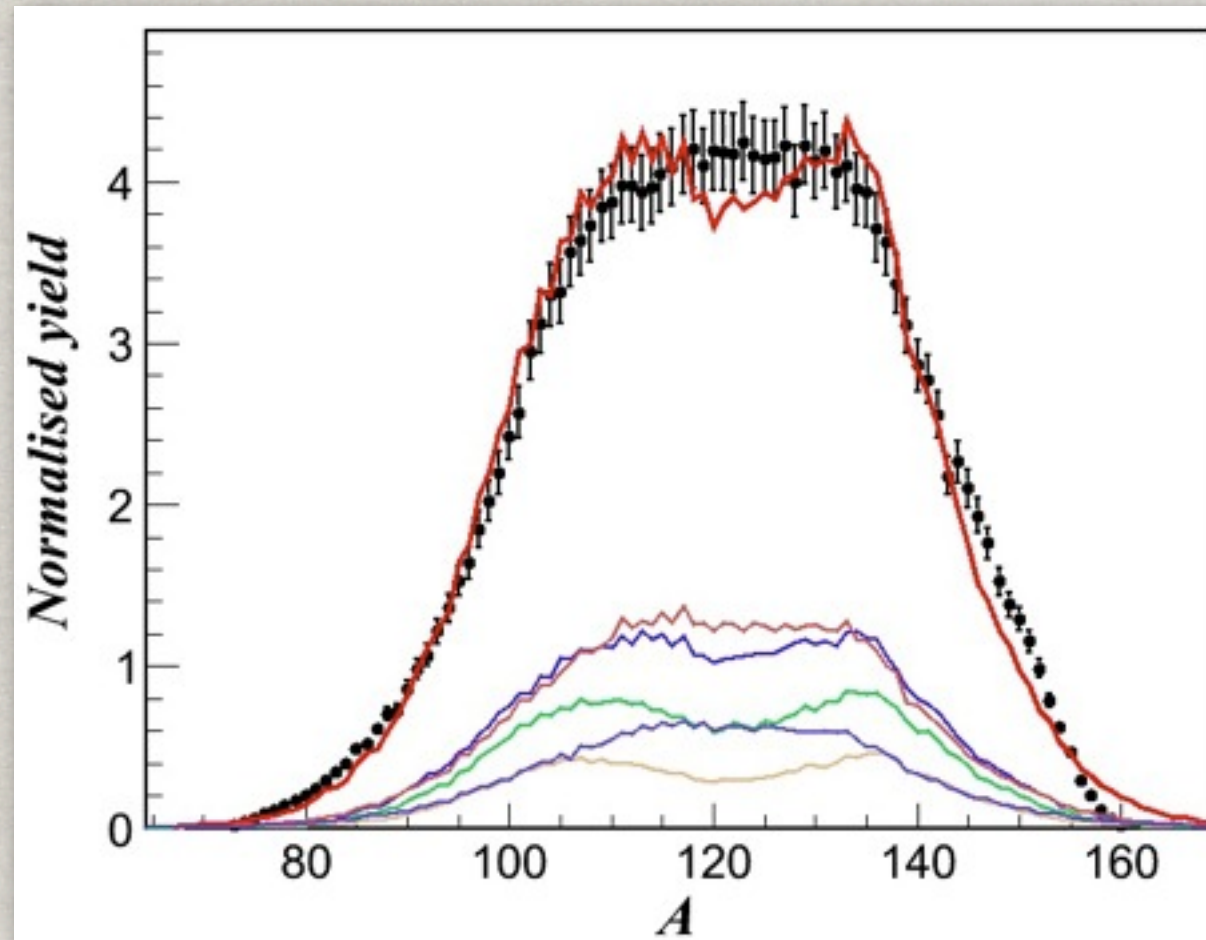


^{238}U (6.1 AMeV) + ^{12}C at VAMOS

^{250}Cf ($E^* \sim 45$ MeV)



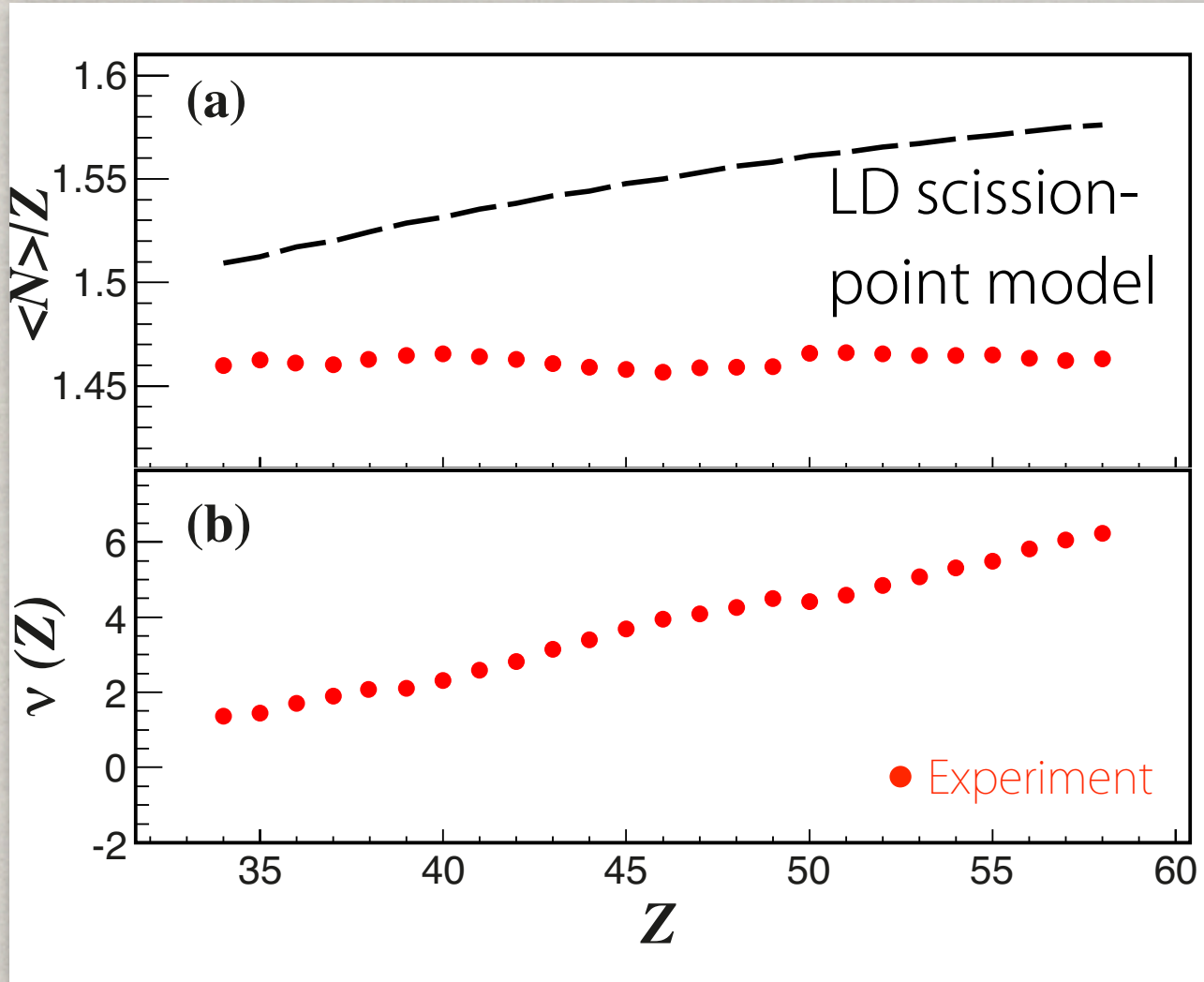
Widths and shapes behave as expected
with small differences.
 $\langle L \rangle$ marks the transition to symmetric fission



solid lines: Code GEF (K.-H. Schmidt & B. Jurado)

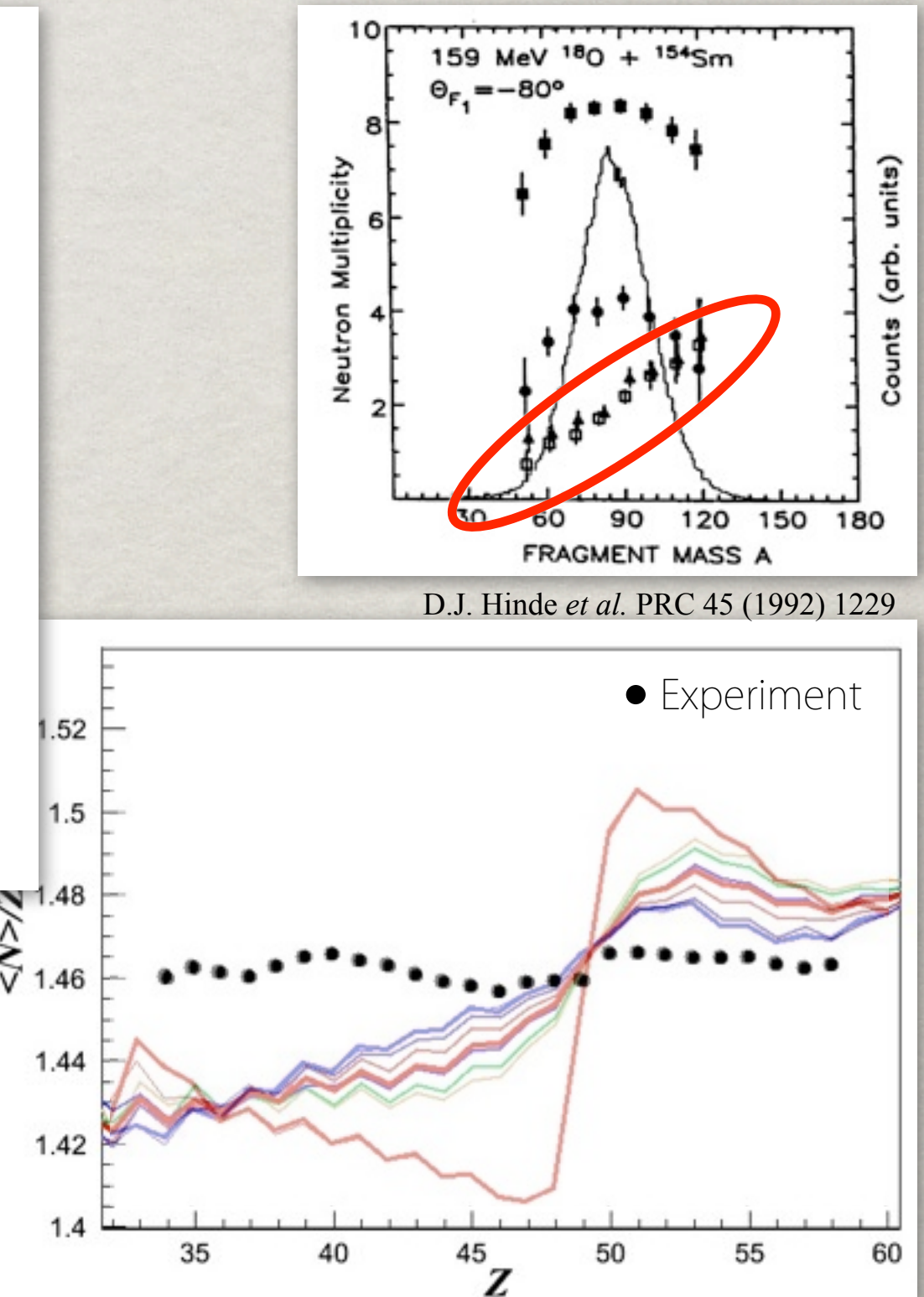
^{238}U (6.1 AMeV) + ^{12}C at VAMOS

^{250}Cf ($E^* \sim 45$ MeV)



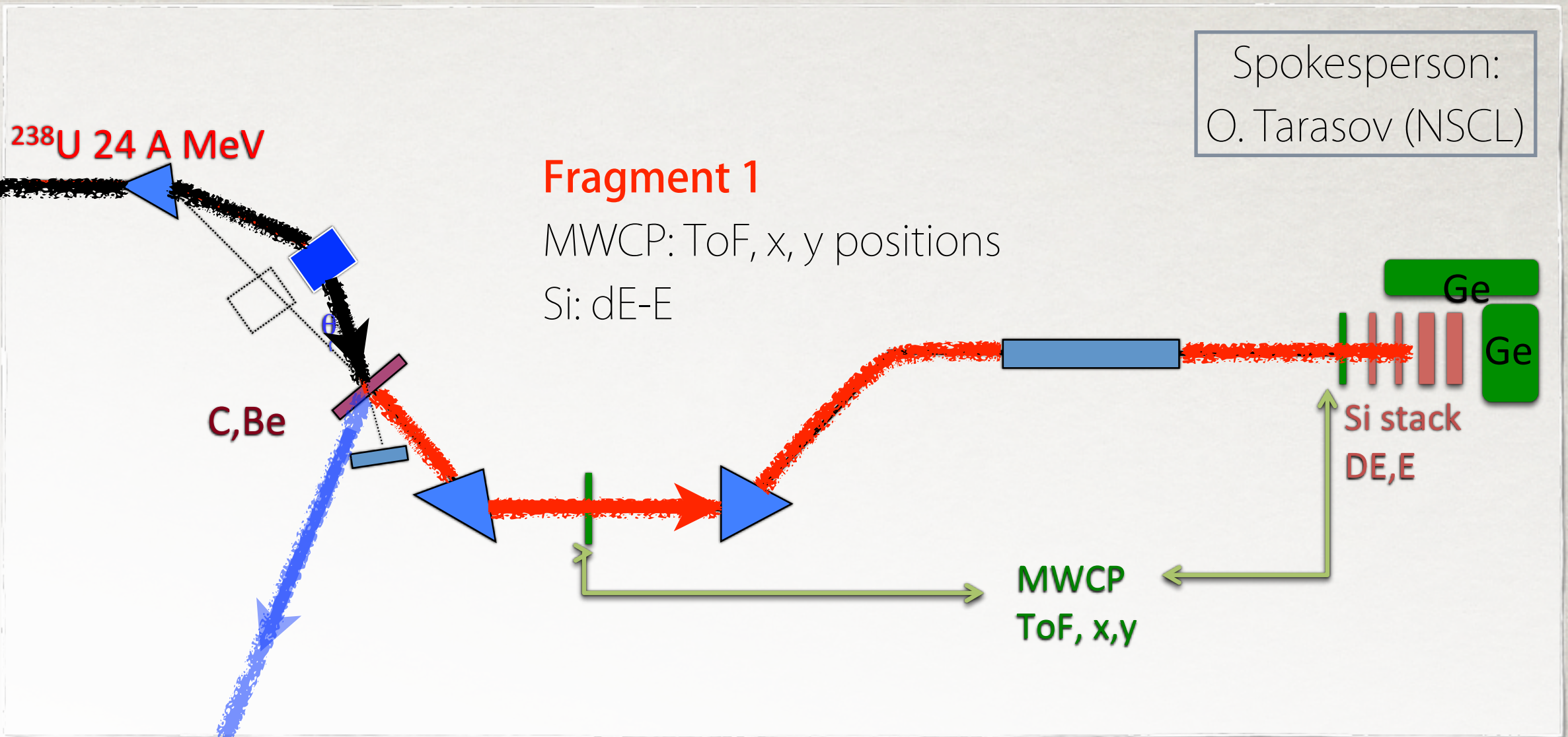
LD scission-point model
 $E_{\text{tot}} = E_{\text{LD}}(Z_1, A_1) + E_{\text{LD}}(Z_2, A_2)$

- no polarization at high E^*
- cannot be reproduced with multi-chance fission and/or $\langle L \rangle$ influence.



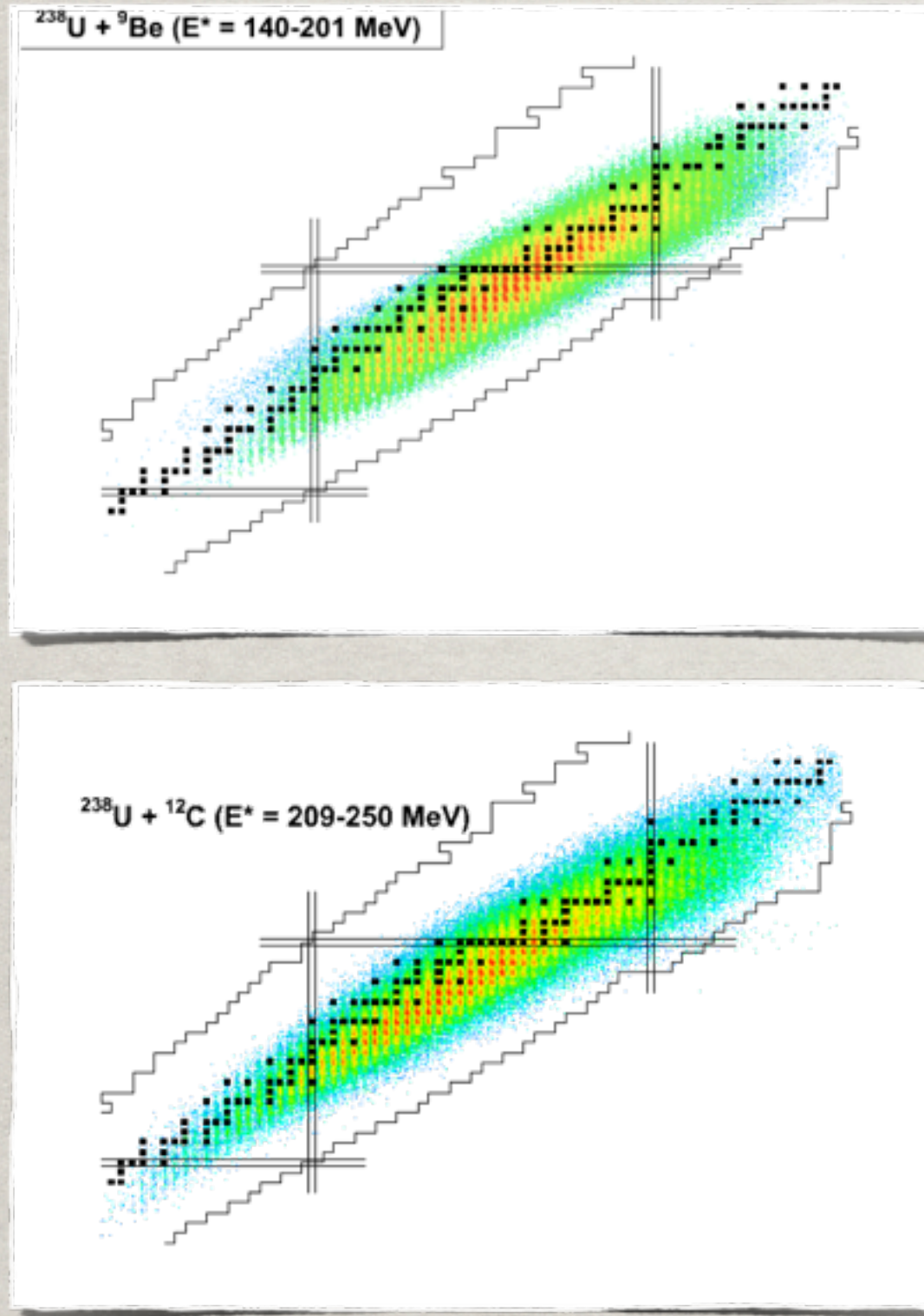
^{238}U (24 AMeV) + $^{12}\text{C}/^9\text{Be}$ at LISE

- Setup based on inverse kinematics
- Fusion-fission at different E^*

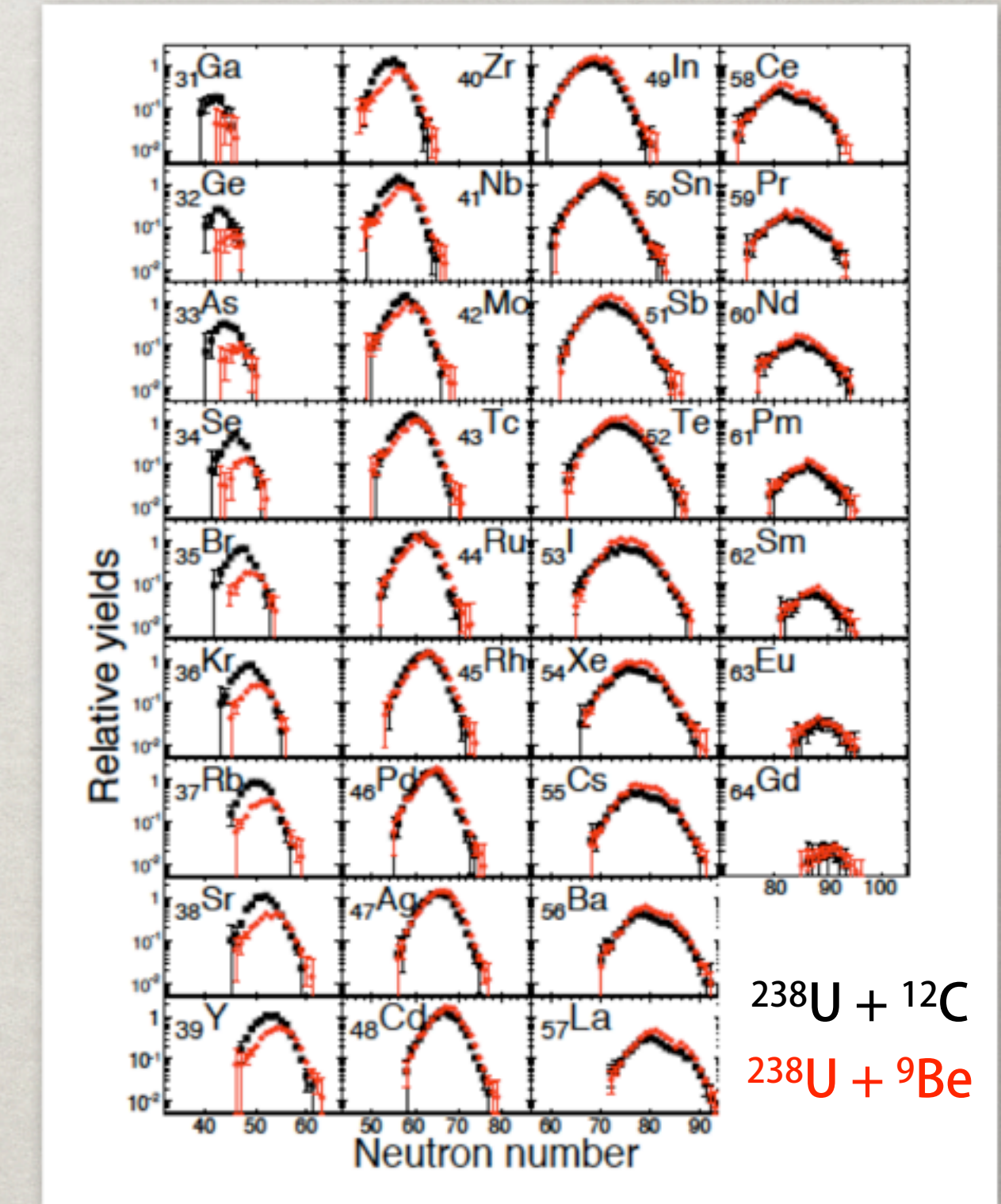


Fragment's observables: Z, A, q, angles, velocity, gammas.

^{238}U (24 AMeV) + $^{12}\text{C}/^9\text{Be}$ at LISE



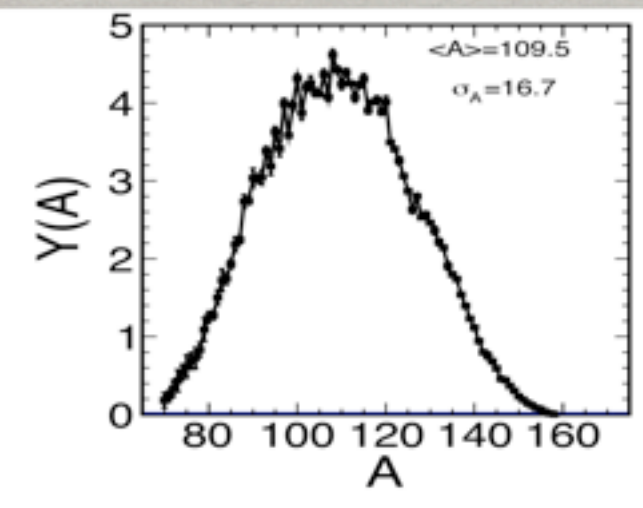
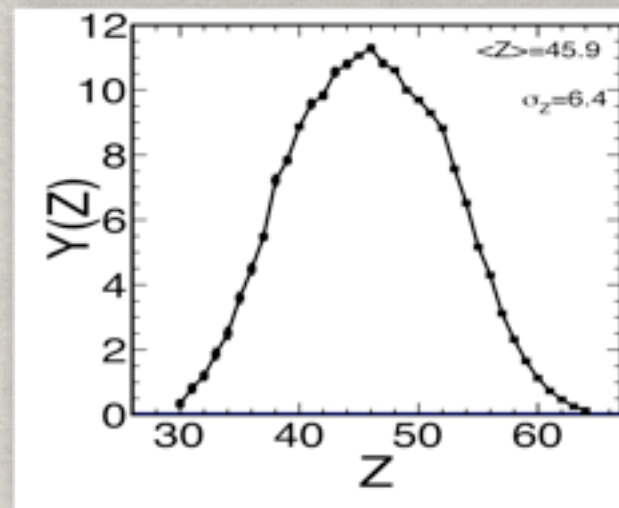
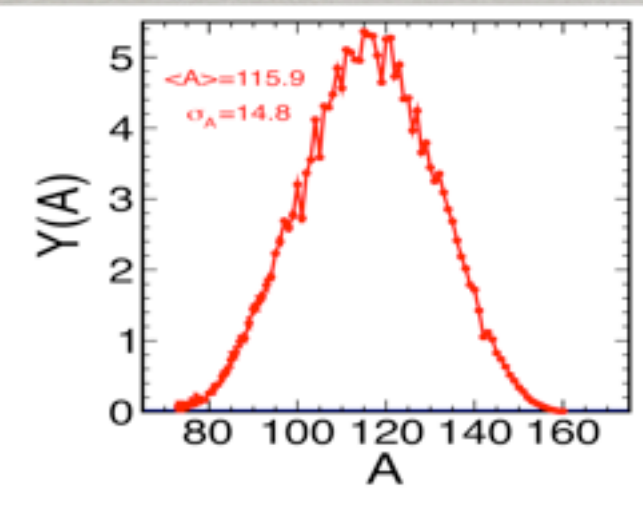
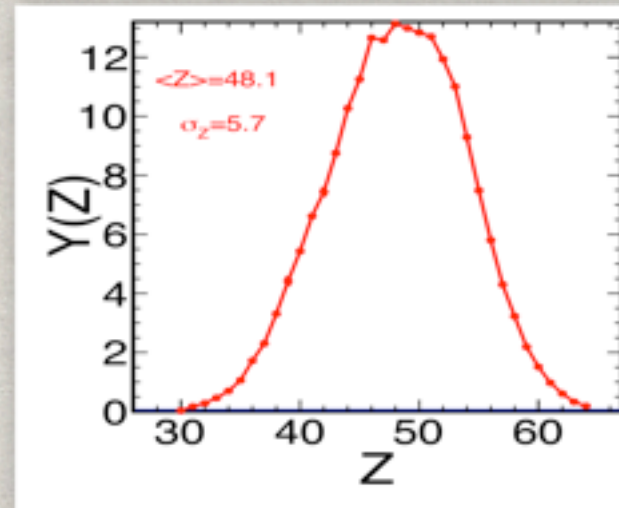
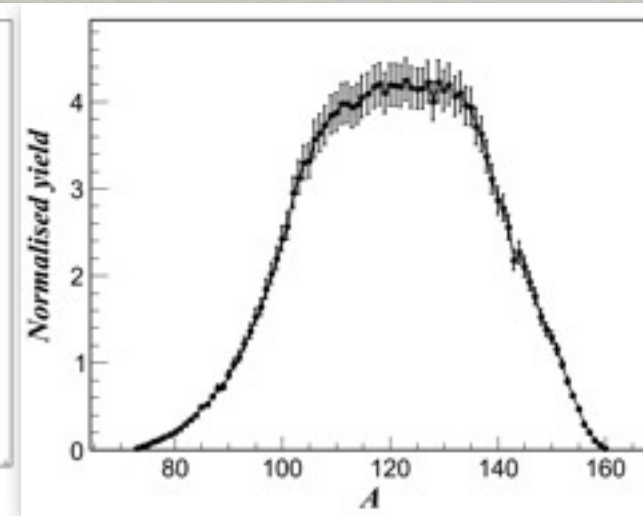
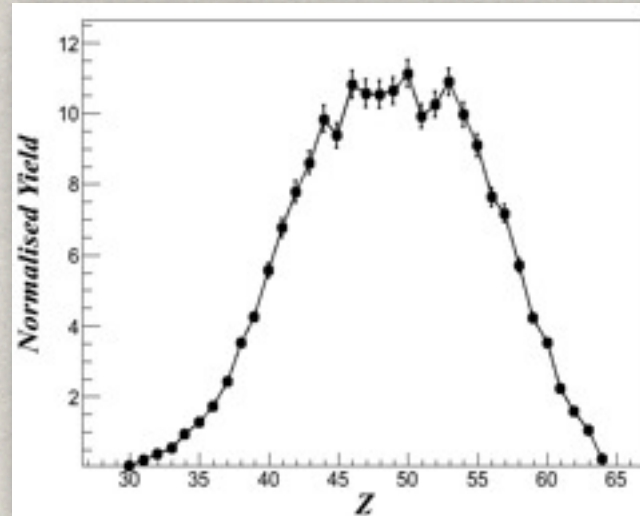
$^{132}\text{Sn} \sim 10 \text{ pps}$



O. Delaune *et al.*, to be published

$^{238}\text{U} + ^{12}\text{C}/^9\text{Be}$

Fusion-fission summary



^{250}Cf ^{238}U (6.1 AMeV) + ^{12}C
 $E^* = 45$ MeV
 $\langle L \rangle \sim 15$
 $2^* \langle Z \rangle = 98$ $2^* \langle A \rangle = 243$ ($v \sim 7$)

^{247}Cm ^{238}U (24 AMeV) + ^9Be
 $E^* = 200 - 150$ MeV
 $\langle L \rangle \sim 75$
 $2^* \langle Z \rangle = 96$ $2^* \langle A \rangle = 232$ ($v \sim 15$)

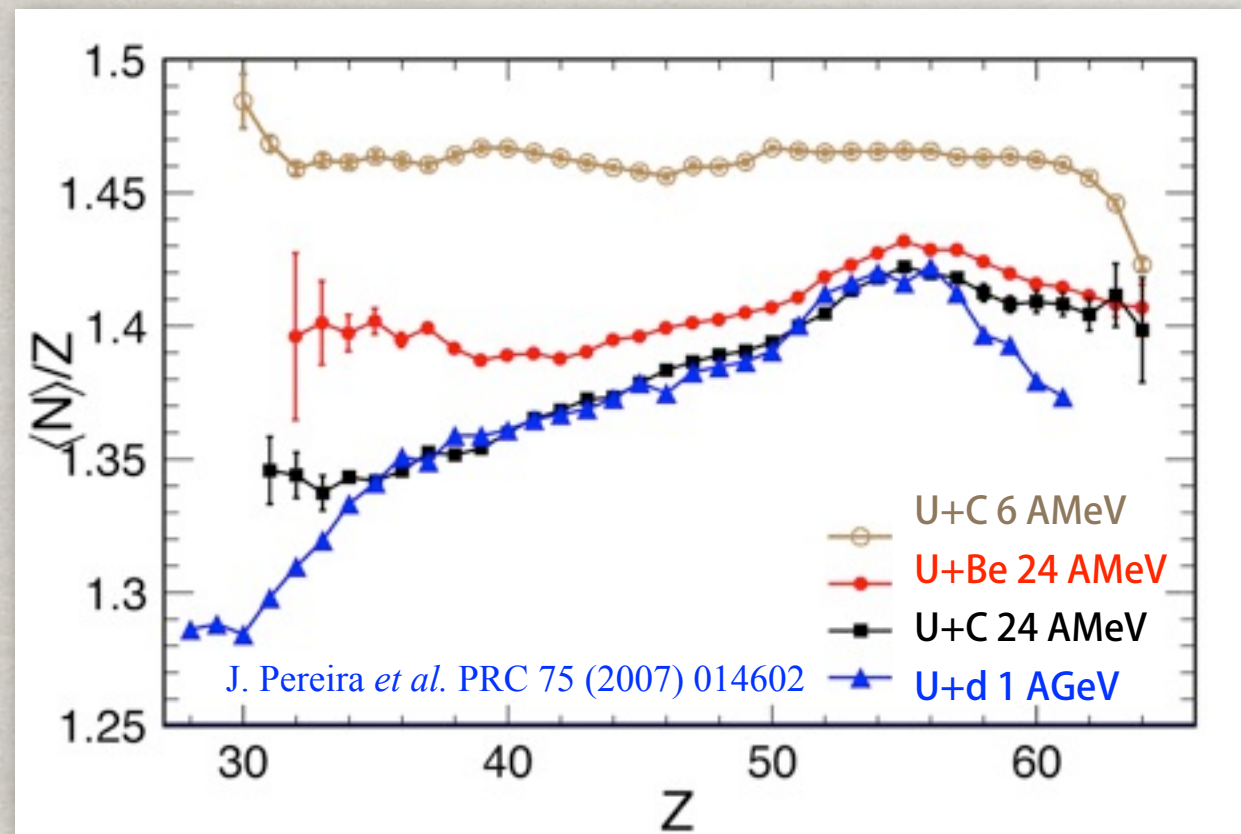
~~^{250}Cf~~ ^{238}U (24 AMeV) + ^{12}C
 $E^* = 250 - 200$ MeV
 $\langle L \rangle \sim 95$
 $2^* \langle Z \rangle = 92$ $2^* \langle A \rangle = 219$ ($v \sim ?$)

no fusion occurs

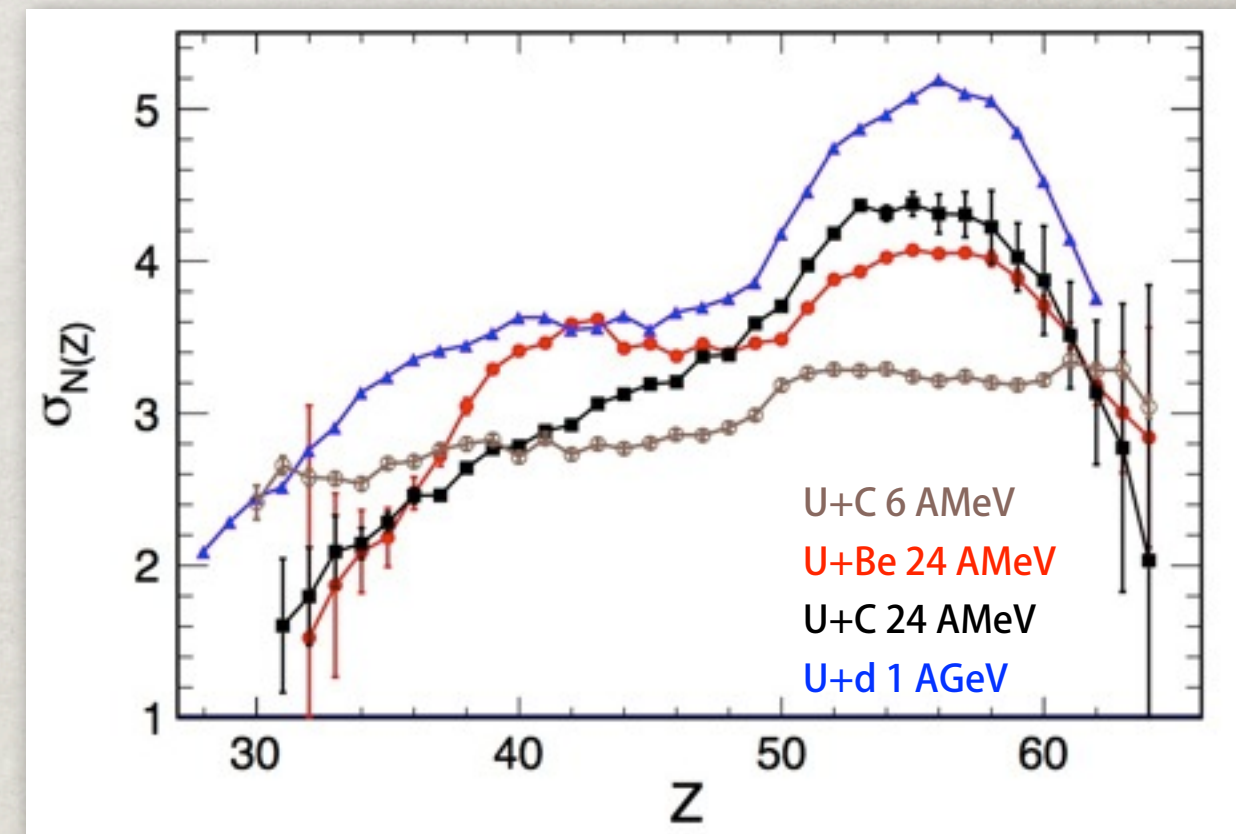
$^{238}\text{U} + ^{12}\text{C}/^9\text{Be}$

Fusion-fission summary

polarisation



width of isotopic distribution



O. Delaune *et al.*, to be published

- As E^* diminishes, $\langle N \rangle/Z$ becomes flat in U+C @ 6 AMeV (!!)
- U+Be recovers some shell influence (maybe due to evaporation)
- U+C @ 24 AMeV is remarkably similar to spallation reactions

Summary and conclusions

- The study of transfer- and fusion-induced fission in inverse kinematics allows the **access to observables not available so far**.
- We have shown A , Z , $\langle N \rangle/Z$, and **velocity** distributions for ^{250}Cf , ^{247}Cm , and ^{240}Pu , and their evolution with E^* and the reaction mechanism.
- The ^{240}Pu measured distributions are in agreement with their expected behaviour.
- ^{250}Cf with $E^*=45$ MeV shows **unexpected features** in $\langle N \rangle/Z$, velocity, and isotopic distributions.
- The results on ^{250}Cf reveal the **need for a better understanding** of the fission process, post-saddle.
- The study of the isotopic distributions of fission fragments proves to be a valid tool to extract **new information on the fission dynamics**.